KA-TP-13-1997

Precision tests of the electroweak theory

W. Hollik

Institut für Theoretische Physik, Universität Karlsruhe, D-76128 Karlsruhe, Germany

Abstract. In this review we give a discussion of the structure of the Standard Model and its quantum corrections for testing the electroweak theory at present and future colliders. After a sort summary of the tree level structure of the Standard Model we outline the calculation of physcial quantities at the quantum level. Concrete applications are given to the vector boson mass interdependence and the Z resonance. Finally we show a comparision of the Standard Model prediction for the electroweak precision observables with the most recent experimental data.

Short title: Precision tests of the electroweak theory

August 11, 1997

Precision tests of the electroweak theory

W. Hollik

Institut für Theoretische Physik, Universität Karlsruhe, D-76128 Karlsruhe, Germany

Abstract. In this review we give a discussion of the structure of the Standard Model and its quantum corrections for testing the electroweak theory at present and future colliders. After a sort summary of the tree level structure of the Standard Model we outline the calculation of physcial quantities at the quantum level. Concrete applications are given to the vector boson mass interdependence and the Z resonance. Finally we show a comparision of the Standard Model prediction for the electroweak precision observables with the most recent experimental data.

1. Introduction

The e^+e^- colliders LEP and SLC, in operation since summer 1989, have collected an immense material on electroweak precision data from measurements around the Z resonance. In parallel, from the proton-antiproton collider Tevatron the W boson properties have been determined with better and better accuracy, and the experimental discovery of the top quark has been reported with steadily rising precision in its mass. The ongoing experiments at LEP 2 and the near future Tevatron upgrade will also for the coming years support us with further increase in precision, in particular on the mass of the W and the top, and SLC will continue in improving the already obtained impressive accuracy in the electroweak mixing angle. This impressive experimental program together with the theoretical activities to provide accurate predictions from the Standard Model of elementary particle physics has formed the era of electroweak precison tests and will keep it alive for the forthcoming years.

The theory of the electroweak interaction [1, 2, 3, 4] is a gauge invariant quantum field theory with the symmetry group $SU(2) \times U(1)$ spontaneously broken by the Higgs mechanism. The possibility to perform perturbative calculations for observable quantities in terms of a few input parameters is substantially based on the renormalizability of this class of theories [5]. The input parameters cannot be predicted but have to be taken from experiment. In the electrowek Standard Model essentially three free parameters are required to describe the gauge bosons $\gamma, W^{\pm}, Z$ and their interactions with the fermions. For a comparison between theory and experiment hence three independent experimental input data are required. The most natural choice is given by the electromagnetic fine structure constant α, the muon decay constant (Fermi constant) G_μ, and the mass of the Z boson which has meanwhile been measured with the same accuracy as G_μ [6]. Other measurable quantities are predicted in terms of the input data. Each additional precision experiment which allows the detection of small deviations from the lowest order predictions can be considered a test of the electroweak theory at the quantum level. In the Feynman

graph expansion of the scattering amplitude for a given process the higher order terms show up as diagrams containing closed loops. The lowest order amplitudes could also be derived from a corresponding classical field theory whereas the loop contributions can only be obtained from the quantized version. The renormalizability of the Standard Model ensures that it retains its predictive power also in higher orders. The higher order terms, commonly called radiative corrections, are the quantum effects of the electroweak theory. They are complicated in their concrete form, but they are finally the consequence of the basic Lagrangian with a simple structure. The quantum corrections contain the self-coupling of the vector bosons as well as their interactions with the Higgs field and the top quark, and provide the theoretical basis for electroweak precision tests. Assuming the validity of the Standard model, the presence of the top quark and the Higgs boson in the loop contributions to electroweak observables allows an indirect access to their mass ranges from precision measurements of precision observables.

The present generation of high precision experiments hence imposes stringent tests on the Standard Model. Besides the impressive achievements in the determination of the Z boson parameters [6] and the W mass [7, 6], the most important step has been the discovery of the top quark at the Tevatron [8] with the mass determination $m_t = 175.6 \pm 5.5$ GeV, which coincides perfectly with the indirectly obtained mass range via the radiative corrections. Moreover, with the top mass as an additional precise experimental data point one now can fully exploit the sensitivity to the Higgs mass.

The high experimental sensitivity in the electroweak observables, at the level of the quantum effects, requires the highest standards on the theoretical side as well. A sizeable amount of work has contributed over the last few years to a steadily rising improvement of the standard model predictions pinning down the theoretical uncertainties to a level sufficiently small for the current interpretation of the precision data (for a status report see [9]). Future increase in the experimental accuracy, however, will need also more theoretical effort.

The lack of direct signals from new physics beyond the Standard Model makes the high precision experiments also a unique tool in the search for indirect effects: through possible deviations of the experimental results from the theoretical predictions of the minimal Standard Model. Since such deviations are expected to be small, it is decisive to have the the standard loop effects in the precision observables under control.

In this review we give a discussion of the structure of the Standard Model and its quantum corrections for testing the electroweak theory at present and future colliders. After a short summary of the tree level structure of the Standard Model in section 2 we outline the calculation of physcial quantities at the quantum level. Concrete applications are given to the vector boson mass interdependence and the Z resonance in e^+e^- in sections 4 and 5. Finally, in section 6 we show a comparision of the Standard Model prediction for the electroweak precision observables with the most recent experimental data.

2. The electroweak Standard Model at the tree-level

The standard model of the fundamental electroweak interactions of elementary particles is derived from the principle of local gauge invariance based on the group $SU(2)\times U(1)$. Thereby, the fundamental spin $1/2$ matter fields are classified as families with left-handed $SU(2)$ doublets and right-handed singlets:

$$\begin{pmatrix} \nu_e \\ e \end{pmatrix}_L, \quad \begin{pmatrix} \nu_\mu \\ \mu \end{pmatrix}_L, \quad \begin{pmatrix} \nu_\tau \\ \tau \end{pmatrix}_L, \quad e_R, \quad \mu_R, \quad \tau_R$$

$$\begin{pmatrix} u \\ d \end{pmatrix}_L, \quad \begin{pmatrix} c \\ s \end{pmatrix}_L, \quad \begin{pmatrix} t \\ b \end{pmatrix}_L, \quad u_R, \quad d_R, \quad c_R, \cdots$$

They can be characterized by the quantum numbers of the weak isospin I, I_3, and the weak hypercharge Y. Between the quantum numbers classifying the fermions with respect to the group $SU(2) \times U(1)$ and their electric charges Q the Gell-Mann-Nishijima relation

$$Q \;=\; I_3 \;+\; \frac{Y}{2} \tag{1}$$

is valid.

The electroweak gauge fields consist of a triplet of vector fields $W_\mu^{1,2,3}$ and a singlet field B_μ. The isotriplet W_μ^a, $a = 1, 2, 3$, and the isosinglet B_μ yield the field strength tensors

$$\begin{aligned} W^a_{\mu\nu} &= \partial_\mu W^a_\nu - \partial_\nu W^a_\mu + g_2\, \epsilon_{abc}\, W^b_\mu W^c_\nu, \\ B_{\mu\nu} &= \partial_\mu B_\nu - \partial_\nu B_\mu. \end{aligned} \tag{2}$$

g_2 denotes the non-Abelian $SU(2)$ gauge coupling constant and g_1 the Abelian $U(1)$ coupling. From the field tensors (2) the pure gauge field Lagrangian

$$\mathcal{L}_G = -\frac{1}{4}\, W^a_{\mu\nu} W^{\mu\nu,a} - \frac{1}{4}\, B_{\mu\nu} B^{\mu\nu} \tag{3}$$

is constructed according to the basic rules for non-Abelian gauge theories.

For breaking the $SU(2) \times U(1)$ symmetry spontaneously leaving the electromagnetic gauge subgroup $U(1)_{em}$ unbroken, a single complex scalar doublet field $\Phi(x)$ with hypercharge $Y = 1$ is coupled to the gauge fields in terms of the Lagrangian

$$\mathcal{L}_H = (D_\mu \Phi)^+ (D^\mu \Phi) - V(\Phi) \tag{4}$$

with the covariant derivative involving the isospin generators I_a

$$D_\mu = \partial_\mu \;-\; i\, g_2\, I_a W^a_\mu \;+\; i\, \frac{g_1}{2}\, B_\mu\,.$$

The Higgs field self-interaction

$$V(\Phi) = -\mu^2\, \Phi^+ \Phi + \frac{\lambda}{4}\, (\Phi^+ \Phi)^2 \tag{5}$$

is constructed in such a way that it has a non-vanishing vacuum expectation value v, related to the coefficients of the potential V by

$$v = \frac{2\mu}{\sqrt{\lambda}}\,. \tag{6}$$

The field Φ can be written in the following way:

$$\Phi(x) = \begin{pmatrix} \phi^+(x) \\ (v + H(x) + \mathrm{i}\chi(x))/\sqrt{2} \end{pmatrix} = \begin{pmatrix} \phi^+(x) \\ \phi^0(x) \end{pmatrix} \tag{7}$$

where the components H, χ, ϕ^+ now have vacuum expectation values zero. Exploiting the invariance of the Lagrangian one notices that the components ϕ^+, χ can be gauged away which means that they are unphysical (Higgs ghosts or would-be Goldstone bosons). In this particular gauge, the unitary gauge, the Higgs field has the simple form

$$\Phi(x) = \frac{1}{\sqrt{2}} \begin{pmatrix} 0 \\ v + H(x) \end{pmatrix} .$$

The real part of $H(x)$ describes physical neutral scalar particles with mass

$$M_H = \mu\sqrt{2}. \tag{8}$$

The Higgs field components have triple and quartic self couplings following from V, and couplings to the gauge fields via the kinetic term of Eq. (4).

In addition, Yukawa couplings to fermions are introduced in order to make the charged fermions massive. The Yukawa term is conveniently expressed in the doublet field components (7). For one family of leptons and quarks it is given by

$$\begin{aligned} \mathcal{L}_{\text{Yukawa}} &= -\, g_l\, (\overline{\nu}_L\, \phi^+\, l_R \,+\, \overline{l}_R\, \phi^-\, \nu_L \,+\, \overline{l}_L\, \phi^0\, l_R \,+\, \overline{l}_R\, \phi^{0*}\, l_L) \\ &= -\, g_d\, (\overline{u}_L\, \phi^+\, d_R \,+\, \overline{d}_R\, \phi^-\, u_L \,+\, \overline{d}_L\, \phi^0\, d_R \,+\, \overline{d}_R\, \phi^{0*}\, d_L) \\ &\quad -\, g_u\, (-\overline{u}_R\, \phi^+\, d_L \,-\, \overline{d}_L\, \phi^-\, u_R \,+\, \overline{u}_R\, \phi^0\, u_L \,+\, \overline{u}_L\, \phi^{0*}\, u_R) \,. \end{aligned} \tag{9}$$

ϕ^- denotes the hermitian adjoint of ϕ^+.

By $v \neq 0$ fermion mass terms are induced. The Yukawa coupling constants $g_{l,d,u}$ are related to the masses of the charged fermions by

$$m_f = g_f\, \frac{v}{\sqrt{2}} \,. \tag{10}$$

In the unitary gauge the Yukawa Lagrangian is particularly simple:

$$\mathcal{L}_{\text{Yukawa}} \;=\; -\sum_f\, m_f\, \bar{\psi}_f \psi_f \,-\, \sum_f\, \frac{m_f}{v}\, \bar{\psi}_f \psi_f\, H \,. \tag{11}$$

As a remnant of this mechanism for generating fermion masses in a gauge invariant way, Yukawa interactions between the massive fermions and the physical Higgs field occur with coupling constants proportional to the fermion masses.

For describing the interaction between the fundamental fermions and the gauge fields it is convenient to introduce the physical charged boson fields

$$W^\pm_\mu = \frac{1}{\sqrt{2}}\, (W^1_\mu \pm \mathrm{i} W^2_\mu) \tag{12}$$

and the neutral Z boson and photon fields:

$$\begin{aligned} Z_\mu &= \quad \cos\theta_W\, W^3_\mu \,+ \sin\theta_W\, B_\mu \\ A_\mu &= -\sin\theta_W\, W^3_\mu \,+ \cos\theta_W\, B_\mu \end{aligned} \tag{13}$$

As a basic feature of the Higgs mechanism, the masses arise to

$$\begin{aligned} M_W &= \frac{1}{2}\, g_2 v \\ M_Z &= \frac{1}{2}\sqrt{g_1^2 + g_2^2}\, v \end{aligned} \tag{14}$$

and the electroweak mixing angle fulfills the relation

$$\cos\theta_W = \frac{g_2}{\sqrt{g_1^2 + g_2^2}} = \frac{M_W}{M_Z}\,. \tag{15}$$

The fermion-gauge interaction term of the standard model Lagrangian contains the electromagnetic current (summation extends over the fermion fields ψ_f)

$$J_\mu^{\rm em} = \sum_f Q_f\, \bar\psi_f \gamma_\mu \psi_f\,, \tag{16}$$

the weak neutral current

$$J_\mu^{\rm Z} = \sum_f \bar\psi_f \gamma_\mu (v_f - a_f\gamma_5)\psi \tag{17}$$

with the coupling constants

$$\begin{aligned} v_f &= I_3^f - 2Q_f\, \sin^2\theta_W \\ a_f &= I_3^f\,. \end{aligned} \tag{18}$$

(where Q_f and I_3^f denote the charge and the third isospin component of f_L), and the weak charged current

$$J_\mu^+ = \sum_{\ell=e,\mu,\tau} \bar\nu_\ell \gamma_\mu (1-\gamma_5)\ell \;+\; (\bar u, \bar c, \bar t)\gamma_\mu(1-\gamma_5) U_{\rm KM} \begin{pmatrix} u \\ s \\ b \end{pmatrix} \tag{19}$$

(with the Cabibbo-Kobayashi-Maskawa matrix $U_{\rm KM}$ [3]) in the following way:

$$\mathcal{L}_{f-G} = -e\, J_\mu^{\rm em} A^\mu + \frac{g_2}{2\cos\theta_W} J_\mu^{\rm Z} Z^\mu + \frac{g_2}{2\sqrt{2}}(J_\mu^+ W^{\mu-} + \text{h.c.})\,. \tag{20}$$

The electric charge $e = \sqrt{4\pi\alpha}$ can be expressed in terms of the gauge couplings in the following way

$$e = \frac{g_1 g_2}{\sqrt{g_1^2 + g_2^2}} \tag{21}$$

or

$$g_2 = \frac{e}{\sin\theta_W}, \quad g_1 = \frac{e}{\cos\theta_W}. \tag{22}$$

The relations above allow one to replace the original set of electroweak parameters

$$g_2,\; g_1,\; \lambda,\; \mu^2,\; g_f \tag{23}$$

by the equivalent set of more physical parameters

$$e,\ M_W,\ M_Z,\ M_H,\ m_f \tag{24}$$

where each of them is measureable in a suitable experiment.

An additional, very precisely measured, parameter is the Fermi constant G_μ which is the effective 4-fermion coupling constant in the the Fermi model, obtained from the muon lifetime [10]:

$$G_\mu = 1.16639(2) \cdot 10^{-5}\,\mathrm{GeV}^{-2}\,.$$

Consistency of the Standard Model at momentum transfer $q^2 \ll M_W^2$ with the Fermi model requires the identification (see section 4)

$$\frac{G_\mu}{\sqrt{2}} = \frac{e^2}{8 \sin^2\theta_W M_W^2}\,, \tag{25}$$

which allows us to relate the vector boson masses to the parameters α, G_μ, $\sin^2\theta_W$ as follows:

$$\begin{aligned} M_W^2 &= \frac{\pi\alpha}{\sqrt{2}G_\mu} \cdot \frac{1}{\sin^2\theta_W} \\ M_Z^2 &= \frac{\pi\alpha}{\sqrt{2}G_\mu} \cdot \frac{1}{\sin^2\theta_W \cos^2\theta_W} \end{aligned} \tag{26}$$

and thus to establish the tree-level $M_W - M_Z$ interdependence:

$$M_W^2 \left(1 - \frac{M_W^2}{M_Z^2}\right) = \frac{\pi\alpha}{\sqrt{2}G_\mu}\,. \tag{27}$$

These relations will be modified by the higher order quantum effects in a significant way.

In order to describe scattering processes between light fermions in lowest order we can, in most cases, neglect the exchange of Higgs bosons because of their small Yukawa couplings to the light fermions. The standard 4-fermion processes are mediated by the gauge bosons and, sufficient in lowest order, defined by the vertices for the fermions interacting with the vector bosons as given in Eq. (18) In the charged current vertices the elements of the CKM matrix appear

$$U_{KM} = \begin{pmatrix} V_{ud} & V_{us} & V_{ub} \\ V_{cd} & V_{cs} & V_{cb} \\ V_{td} & V_{ts} & V_{tb} \end{pmatrix} \tag{28}$$

which describes family mixing in the quark sector [3]. Its origin is the diagonalization of the quark mass matrices from the Yukawa coupling which appears since quarks of the same charge have different masses. For massless neutrinos no mixing in the leptonic sector is present. Due to the unitarity of U_{KM} the mixing is absent in the neutral current.

For a proper treatment of the charged current vertex at the one-loop level, the matrix U_{KM} has to be renormalized as well. As it was shown in [11], where the renormalization procedure was extended to U_{KM}, the resulting effects are completely negligible for the known light fermions. We therefore skip the renormalization of U_{KM} in our discussion of radiative corrections.

3. Renormalization of one-loop amplitudes

3.1. Basic strategy

In higher order perturbation theory the relations between the formal parameters and measureable quantities are in general different from the tree level relations. The calculation is, moreover, plagued by the appearence of divergences arising from loop integrations. For a mathematically consistent treatment one has to regularize the theory, e.g. by dimensional regularization (performing the calculations in D dimensions) [12]. But then the relations between physical quantities and the parameters, the so-called "bare" parameters, become cutoff dependent. On the other hand, relations between measureable physical quantities, where the parameters drop out, are finite and independent of the cutoff. It is therefore in principle possible to perform tests of the theory in terms of such relations by eliminating the bare parameters [13, 14].

Alternatively, one may replace the bare parameters by renormalized ones by multiplicative renormalization for each bare parameter a_0

$$a_0 = Z_a\, a = a + \delta a \tag{29}$$

with renormalization constants Z_a different from 1 by a higher order term. The renormalized parameters a are finite and fixed by explicit renormalization conditions. The decomposition (29) is to a large extent arbitrary. Only the divergent parts are determined directly by the structure of the divergences of the one-loop amplitudes. The finite parts depend on the choice of the explicit renormalization conditions.

This procedure of parameter renormalization is sufficient to obtain finite S-matrix elements when wave function renormalization for external on-shell particles is included. Off-shell Green functions, however, are not finite by themselves. In order to obtain finite propagators and vertices, the bare fields in $\mathcal{L}$ also have to be redefined in terms of renormalized fields by multiplicative renormalization

$$\phi_0 = Z_\phi^{1/2}\, \phi\,. \tag{30}$$

Expanding the renormalization constants according to

$$Z_i = 1 + \delta Z_i$$

the Lagrangian is split into a "renormalized" Lagrangian and a counter term Lagrangian

$$\mathcal{L}(\phi_0, a_0) = \mathcal{L}(Z_\phi^{1/2}\phi, Z_a a) = \mathcal{L}(\phi, a) + \delta\mathcal{L}(\phi, a, \delta Z_\phi, \delta a) \tag{31}$$

which renders the results for all Green functions in a given order finite.

A simple way to obtain a set of finite Green functions is the "minimal subtraction scheme" [15] where (in dimensional regularization) the singular part of each divergent diagram is subtracted and the parameters are defined at an arbitrary mass scale μ. With slight modifications, this scheme is known as the $\overline{MS}$ scheme, which mainly has been applied in QCD perturbative calculations.

In QED and in the electroweak theory the classical Thomson scattering and the particle masses set natural scales where the parameters can be defined. In QED the favoured renormalization scheme is the on-shell scheme where $e = \sqrt{4\pi\alpha}$

and the electron, muon, ... masses are used as input parameters. The finite parts of the counter terms are fixed by the renormalization conditions that the fermion propagators have poles at their physical masses, and e becomes the $ee\gamma$ coupling constant in the Thomson limit of Compton scattering. In the electroweak Standard Model a distinguished set for parameter renormalization is given in terms of e, M_Z, M_W, M_H, m_f with the masses of the corresponding particles. This electroweak on-shell scheme is the straight-forward extension of the familiar QED renormalization, first proposed by Ross and Taylor [16] and used in many practical applications [25, 17, 18, 19, 20, 21, 22, 23, 24, 26, 27]. The mass of the Higgs boson, as long as it is experimentally unknown, is treated as a free input parameter. The light quark masses can only be considered as effective parameters. In the cases of practical interest they can be replaced in terms of directly measured quantities like the cross section for $e^+e^- \to$ hadrons.

Instead of the set e, M_W, M_Z as basic free parameters one may alternatively use as basic parameters α, G_μ, M_Z [28] or α, G_μ, $\sin^2\theta_W$ with the mixing angle deduced from neutrino-electron scattering [29] or perform the loop calculations in the $\overline{MS}$ scheme [30, 31, 32, 33]. The so-called $*$-scheme [34, 35] is a different way of book-keeping in terms of effective running couplings. Here we follow the on-shell scheme as specified in detail in [25, 26].

3.2. Gauge boson propagators and mass renormalization

Since the S matrix element for any physical process is a gauge invariant quantity it is possible to work in the unitary gauge with no unphysical particles in internal lines. For a systematic treatment of higher order calculations, however, one better refers to a renormalizable gauge. This can be done by adding to the gauge invariant Lagrangian of section 2 a gauge fixing term, for example

$$\mathcal{L}_{fix} = -\frac{1}{2}\left(F_\gamma^2 + F_Z^2 + 2F_+F_-\right) \tag{32}$$

with linear gauge fixings of the 't Hooft type:

$$\begin{aligned} F_\pm &= \frac{1}{\sqrt{\xi^W}}\left(\partial^\mu W_\mu^\pm \mp \mathrm{i}M_W\xi^W\phi^\pm\right) \\ F_Z &= \frac{1}{\sqrt{\xi^Z}}\left(\partial^\mu Z_\mu - M_Z\xi^Z\chi\right) \\ F_\gamma &= \frac{1}{\sqrt{\xi^\gamma}}\,\partial^\mu A_\mu \end{aligned} \tag{33}$$

with arbitrary parameters $\xi^{W,Z,\gamma}$. In this class of 't Hooft gauges, the vector boson propagators have the form

$$\begin{aligned} &\frac{\mathrm{i}}{q^2 - M_V^2}\left(-g^{\mu\nu} + \frac{(1-\xi^V)q^\mu q^\nu}{q^2 - \xi^V M_V^2}\right) = \\ &\frac{\mathrm{i}}{q^2 - M_V^2}\left(-g^{\mu\nu} + \frac{q^\mu q^\nu}{q^2}\right) + \frac{\mathrm{i}\xi^V}{q^2 - \xi^V M_V^2}\,\frac{q^\mu q^\nu}{q^2}\,, \end{aligned} \tag{34}$$

the propagators for the unphysical Higgs fields are given by

$$\frac{\mathrm{i}}{q^2 - \xi^W M_W^2} \quad \text{for} \quad \phi^\pm$$

$$\frac{\mathrm{i}}{q^2 - \xi^Z M_Z^2} \quad \text{for} \quad \chi^0\,, \tag{35}$$

and scalar - vector boson transitions do not occur.

For completion of the renormalizable Lagrangian the Faddeev-Popov ghost term $\mathcal{L}_{gh}$ has to be added [36] in order to balance the undesired effects in the unphysical components introduced by $\mathcal{L}_{fix}$:

$$\mathcal{L}_{gh} = \bar{u}^\alpha(x)\,\frac{\delta F^\alpha}{\delta\theta^\beta(x)}\,u^\beta(x) \tag{36}$$

with ghost fields u^γ, u^Z, $u^\pm$, and $\frac{\delta F^\alpha}{\delta\theta^\beta}$ being the change of the gauge fixing operators (33) under infinitesimal gauge transformations characterized by $\theta^\alpha(x) = \{\theta^a(x),\, \theta^Y(x)\}$.

In the 't Hooft-Feynman gauge ($\xi = 1$) the vector boson propagators (34) become particularly simple: the transverse and longitudinal components, as well as the propagators for the unphysical Higgs fields $\phi^\pm$, χ and the ghost fields $u^\pm$, u^Z have poles which coincide with the masses of the corresponding physical particles $W^\pm$ and Z. For the complete list of Feynman rules and 1-loop self-energies see for example [25].

In the following we work in the $\xi = 1$ gauge and restrict our discussion to the transverse parts $\sim g_{\mu\nu}$ of the self-energies In the electroweak theory, differently from QED, the longitudinal components $\sim q_\mu q_\nu$ of the vector boson propagators do not give zero results in physical matrix elements. But for light external fermions the contributions are suppressed by $(m_f/M_Z)^2$ and can safely be neglected. Writing the self-energies as

$$\Sigma^{W,Z}_{\mu\nu} = g_{\mu\nu}\Sigma^{W,Z} + \cdots \tag{37}$$

with scalar functions $\Sigma^{W,Z}(q^2)$ we have for the 1-loop propagators ($V = W, Z$)

$$D_V^{\mu\nu}(q) = \frac{-\mathrm{i}g^{\mu\sigma}}{q^2 - M_V^2}\left(-\mathrm{i}\,\Sigma^V_{\rho\sigma}\right)\frac{-\mathrm{i}g^{\rho\nu}}{q^2 - M_V^2} = \frac{-\mathrm{i}g^{\mu\nu}}{q^2 - M_V^2}\left(\frac{-\Sigma^V(q^2)}{q^2 - M_V^2}\right) \tag{38}$$

(the factor $-\mathrm{i}$ in the self energy insertion is a convention). Besides the fermion loop contributions in the electroweak theory there are also the non-Abelian gauge boson loops and loops involving the Higgs boson. The Higgs boson thus enters the 4-fermion amplitudes as an experimentally unknown object at the level of radiative corrections with its mass to be treated as an additional free parameter. In the graphical representation, the self-energies for the vector bosons denote the sum of all the diagrams with virtual fermions, vector bosons, Higgs and ghost loops.

Resumming all self energy-insertions yields a geometrical series for the dressed propagators:

$$\begin{aligned}&\frac{-\mathrm{i}g_{\mu\nu}}{q^2 - M_V^2}\left[1 + \left(\frac{-\Sigma^V}{q^2 - M_V^2}\right) + \left(\frac{-\Sigma^V}{q^2 - M_V^2}\right)^2 + \cdots\right]\\ &= \frac{-\mathrm{i}g_{\mu\nu}}{q^2 - M_V^2 + \Sigma^V(q^2)}\,.\end{aligned} \tag{39}$$

The locations of the poles in the propagators are shifted by the self-energies. Consequently, the principal step in *mass renormalization* consists in a re-interpretation of the parameters: the masses in the Lagrangian cannot be the physical masses of W and Z but are the "bare masses" related to the physical masses M_W, M_Z by

$$\begin{aligned} M_W^{0\,2} &= M_W^2 + \delta M_W^2 \\ M_Z^{0\,2} &= M_Z^2 + \delta M_Z^2 \end{aligned} \tag{40}$$

with counterterms of 1-loop order. The dressed propagators according to this prescription are given by

$$\frac{-\mathrm{i}g_{\mu\nu}}{q^2 - M_V^{0\,2} + \Sigma^V(q^2)} = \frac{-\mathrm{i}g_{\mu\nu}}{q^2 - M_V^2 - \delta M_V^2 + \Sigma^V(q^2)}\,. \tag{41}$$

instead of Eq. (39). The renormalization conditions which ensure that $M_{W,Z}$ are the physical masses fix the mass counterterms to be

$$\begin{aligned} \delta M_W^2 &= \mathrm{Re}\,\Sigma^W(M_W^2) \\ \delta M_Z^2 &= \mathrm{Re}\,\Sigma^Z(M_Z^2)\,. \end{aligned} \tag{42}$$

In this way, two of our input parameters and their counterterms have been defined. †

3.3. Charge renormalization

Our third input parameter is the electromagnetic charge e. The electroweak *charge renormalization* is very similar to that in pure QED. As in QED, we want to maintain the definition of e as the classical charge in the Thomson cross section

$$\sigma_{\mathrm{Th}} = \frac{e^4}{6\pi\, m_e^2}\,.$$

Accordingly, the Lagrangian carries the bare charge $e_0 = e + \delta e$ with the charge counter term δe of 1-loop order. The charge counter term δe has to absorb the electroweak loop contributions to the $ee\gamma$ vertex in the Thomson limit. This charge renormalization condition is simplified by the validity of a generalization of the QED Ward identity [38] which implies that those corrections related to the external particles cancel each other. Thus for δe only two universal contributions are left [we use $s_W = \sin\theta_W$, $c_W = \cos\theta_W$ as abbreviations]:

$$\frac{\delta e}{e} = \frac{1}{2}\,\Pi^\gamma(0) - \frac{s_W}{c_W}\,\frac{\Sigma^{\gamma Z}(0)}{M_Z^2}\,. \tag{43}$$

The first one, quite in analogy to QED, is given by the vacuum polarization of the photon. But now, besides the fermion loops, it contains also bosonic loop diagrams from W^+W^- virtual states and the corresponding ghosts. The second term contains the mixing between photon and Z, in general described as a mixing propagator with $\Sigma^{\gamma Z}$ normalized as

$$D^{\mu\nu}_{\gamma Z} = \frac{-\mathrm{i}g^{\mu\nu}}{q^2}\left(\frac{-\Sigma^{\gamma Z}(q^2)}{q^2 - M_Z^2}\right)\,.$$

† Strictly speaking, the masses defined in this way are not the real parts of the S matrix poles. These can be introduced by mass renormalization conditions differing from the ones given here by a two-loop term including the width of the unstable particles [37].

The fermion loop contributions to $\Sigma^{\gamma Z}$ vanish at $q^2 = 0$; only the non-Abelian bosonic loops yield $\Sigma^{\gamma Z}(0) \neq 0$.

To be more precise, the charge renormalization as discussed above, is a condition only for the vector coupling constant of the photon. The axial coupling vanishes for on-shell photons as a consequence of the Ward identity.

From the photon self-energy

$$\Sigma^{\gamma}(q^2) = q^2\,\Pi^{\gamma}(q^2)$$

no mass term arises for the photon since, besides the fermion loops, also the bosonic loops behave like

$$\Sigma^{\gamma}_{\rm bos}(q^2) \simeq q^2\,\Pi^{\gamma}_{\rm bos}(0) \to 0$$

for $q^2 \to 0$ leaving the pole at $q^2 = 0$ in the propagator. The absence of mass terms for the photon in all orders is a consequence of the unbroken electromagnetic gauge invariance.

3.4. Electroweak parameter shifts

We can now discuss the contributions to the electroweak parameter shifts at the 1-loop level via the renormalization procedure induced by the counter terms for the electric charge and for the electroweak mixing angle. Since these counter terms are universal, they appear everywhere where in the lowest order expressions e resp. $\sin^2\theta_W$ is present. The shifts by the counter terms are not finite. However, their finite parts contain large terms from the subclass of fermion loops to the relations between the physical parameters.

$\Delta\alpha$ and effective electromagnetic charge:

The charge counter term in Eq. (43) contains the photon vacuum polarization at $q^2 = 0$. In the fermionic contribution vacuum polarization we split off the subtracted part evaluated at M_Z^2:

$$\begin{aligned}\Pi^{\gamma}(0) =& -\,{\rm Re}\Pi^{\gamma}(M_Z^2) + \Pi^{\gamma}(0) + {\rm Re}\,\Pi^{\gamma}(M_Z^2)\\ =& -\,{\rm Re}\,\hat{\Pi}^{\gamma}(M_Z^2) + {\rm Re}\,\Pi^{\gamma}(M_Z^2)\,.\end{aligned} \tag{44}$$

The subtracted finite quantity $\hat{\Pi}^{\gamma}(M_Z^2)$ can be split into a leptonic and a hadronic part:

$${\rm Re}\,\hat{\Pi}^{\gamma}(M_Z^2) = {\rm Re}\,\hat{\Pi}^{\gamma}_{\rm lept}(M_Z^2) + {\rm Re}\,\hat{\Pi}^{\gamma}_{\rm had}(M_Z^2)\,.$$

Heavy fermions decouple; the top quark yields only a small contribution

$$\hat{\Pi}^{\gamma}_{\rm top}(M_Z^2) \simeq \frac{\alpha}{\pi}\,Q_t^2\,\frac{M_Z^2}{5\,m_t^2} \tag{45}$$

which has not been included in $\hat{\Pi}^{\gamma}_{\rm had}$. Whereas the leptonic content can easily be obtained from

$${\rm Re}\,\hat{\Pi}^{\gamma}_{\rm lept}(M_Z^2) = \sum_{l=e,\mu,\tau}\frac{\alpha}{3\pi}\left(\frac{5}{3} - \log\frac{M_Z^2}{m_l^2}\right) + O\left(\frac{m_l^2}{M_Z^2}\right), \tag{46}$$

no light quark masses are available as reasonable input parameters for the hadronic content. Instead, the 5 flavor contribution to $\hat{\Pi}^{\gamma}_{\rm had}$ can be derived from experimental data with the help of a dispersion relation

$$\hat{\Pi}^{\gamma}_{\rm had}(M_Z^2) = \frac{\alpha}{3\pi}\, M_Z^2 \int_{4m_\pi^2}^{\infty} ds' \, \frac{R^\gamma(s')}{s'(s' - M_Z^2 - i\varepsilon)} \tag{47}$$

with

$$R^\gamma(s) = \frac{\sigma(e^+e^- \to \gamma^* \to \text{hadrons})}{\sigma(e^+e^- \to \gamma^* \to \mu^+\mu^-)}$$

as an experimental quantity up to a scale s_1 and applying perturbative QCD for the tail region above s_1. Using e^+e^- data for the energy range below 40 GeV and perturbative QCD for the high energy tail, the recent updates [43, 44] yield

$$\mathrm{Re}\,\hat{\Pi}^{\gamma}_{\rm had}(M_Z^2) = -0.0280 \pm 0.0007 \tag{48}$$

and thus confirm the the previous value [45] with an improved accuracy. The error is almost completely due to the experimental data. Other determinations [46, 47, 48] agree within one standard deviation. Combining this result with the leptonic part one obtains the total contribution from the light fermions

$$\mathrm{Re}\,\hat{\Pi}^{\gamma}(M_Z^2)_{\rm ferm} = -0.0593 \pm 0.0007\,.$$

This finite quantity is independent of the structure of the electroweak model. It corresponds to a QED induced shift in the electromagnetic fine structure constant

$$\alpha \;\to\; \alpha(1 + \Delta\alpha) \quad \text{with} \quad \Delta\alpha = -\,\mathrm{Re}\,\hat{\Pi}^{\gamma}_{\rm ferm}(M_Z^2) \tag{49}$$

which can be resummed according to the renormalization group accommodating all the leading logarithms of the type $\alpha^n \log^n(M_Z/m_f)$. The result can be interpreted as an effective fine structure constant at the Z mass scale:

$$\alpha(M_Z^2) \;=\; \frac{\alpha}{1 - \Delta\alpha} \;=\; \frac{1}{128.89 \pm 0.09}\,. \tag{50}$$

It corresponds to a resummation of the iterated 1-loop vacuum polarization from the light fermions to all orders.

The ρ-parameter:

The ρ-parameter

$$\rho = \frac{M_W^2}{\cos^2\theta_W M_Z^2} \tag{51}$$

which in the Standard Model is unity at the tree level, gets a deviation $\Delta\rho$ from 1 by radiative corrections. ρ has been defined as the ratio of the neutral to the charged current strength in neutrino scattering [39]. It is modified by the quantum correction

$$\Delta\rho = \frac{\Sigma^Z(0)}{M_Z^2} - \frac{\Sigma^W(0)}{M_W^2} \tag{52}$$

which is finite as far as only heavy fermion terms are considered. A general doublet of fermions with masses m_1, m_2 causes a shift of ρ by [39, 40]

$$\Delta\rho \;=\; N_C\, \frac{\alpha}{16\pi s_W^2 c_W^2 M_Z^2} \left(m_1^2 + m_2^2 - \frac{2m_1^2 m_2^2}{m_1^2 - m_2^2} \log\frac{m_1^2}{m_2^2} \right) . \tag{53}$$

For the (t,b)-doublet, neglecting m_b, one obtains ($N_C = 3$):

$$\Delta\rho = N_C \, \frac{\alpha}{16\pi s_W^2 c_W^2} \, \frac{m_t^2}{M_Z^2} \, . \tag{54}$$

This contribution to $\Delta\rho$ also constitutes a large shift for the electroweak mixing angle following from the expansion of the bare mixing angle

$$s_W^{0\,2} = 1 - \frac{M_W^2 + \delta M_W^2}{M_Z^2 + \delta M_Z^2} \; = \; s_W^2 + c_W^2 \left(\frac{\delta M_Z^2}{M_Z^2} - \frac{\delta M_W^2}{M_W^2} \right) \tag{55}$$

since there are no other terms $\sim m_t^2$ in the mass counter terms $\delta M_Z^2, \delta M_W^2$ besides those which are q^2-independent, hence leading to:

$$\frac{\delta M_Z^2}{M_Z^2} - \frac{\delta M_W^2}{M_W^2} \simeq \frac{\Sigma^Z(0)}{M_Z^2} - \frac{\Sigma^W(0)}{M_W^2} \; = \; \Delta\rho \, . \tag{56}$$

Here we have introduced the abbreviations

$$c_W^2 = \frac{M_W^2}{M_Z^2}, \quad s_W^2 = 1 - c_W^2 \, . \tag{57}$$

There is also a Higgs contribution to $\Delta\rho$ which, however, is not UV finite by itself when derived from the diagrams involving the physical Higgs boson only. The M_H-dependence for large Higgs masses M_H is only logarithmic [41]:

$$\Delta\rho_{\rm H} \simeq \frac{g_2^2}{16\pi^2} \cdot \frac{3 s_W^2}{4 c_W^2} \, \log \frac{M_H^2}{M_W^2} + \cdots \tag{58}$$

In the limit $s_W^2 \to 0, M_Z \to M_W$, where the $U(1)_Y$ is switched off, one finds $\Delta\rho_{\rm H} = 0$. This is the consequence of the global $SU(2)_R$ symmetry of the Higgs Lagrangian ('custodial symmetry'), which is broken by the $U(1)_Y$ group. $\Delta\rho_{\rm H}$ is thus a measure of the $SU(2)_R$ breaking by the weak hypercharge.

In contrast to the top term $\sim m_t^2$, the Higgs boson enters the shift of $\sin^2\theta_W$ not exclusively through $\Delta\rho$. There are additional M_H-dependent terms in $\delta M_Z^2, \delta M_W^2$ besides the ones in $\Sigma^W(0)$ and $\Sigma^Z(0)$. The same remark holds for logarithmic top terms $\sim \log(m_t/M_W)$ which are not present in $\Delta\rho$.

The $M_W - M_Z$ interdependence:

Incorporating the parameter shifts

$$\alpha \to \alpha(1 + \Delta\alpha), \quad s_W^2 \to s_W^2 + c_W^2 \Delta\rho$$

into the tree-level relation (27) we obtain the approximate correlation at 1-loop

$$M_W^2 \left(1 - \frac{M_W^2}{M_Z^2} \right) = \frac{\pi\alpha}{\sqrt{2} G_\mu} \left(1 + \Delta\alpha - \frac{c_W^2}{s_W^2} \Delta\rho + \cdots \right) \tag{59}$$

between the vector boson masses and the other electroweak parameters α and G_μ, taking into account the large contributions from light and heavy fermions. The ellipses indicate the residual terms belonging to the full calculation discussed in the next section.

The neutral current couplings:

In a similar way as done above, we obtain a universal shift in the overall normalization of the NC coupling constants in Eq.s (18,20)

$$\begin{aligned}\frac{e}{2s_W c_W} &\to \frac{e}{2s_W c_W}\left[1+\frac{1}{2}\left(\Delta\alpha - \frac{c_W^2-s_W^2}{s_W^2}\Delta\rho\right)\right] \\ &= (\sqrt{2}G_\mu M_Z^2)^{1/2}\left[1+\frac{\Delta\rho}{2}\right] \\ &\to (\sqrt{2}G_\mu M_Z^2\rho_f)^{1/2} \end{aligned} \tag{60}$$

The complete expressions for the normalization factor

$$\rho_f = 1 + \Delta\rho + \cdots$$

and the effective mixing angle

$$s_f^2 = s_W^2 + c_W^2\Delta\rho + \cdots$$

in the Zff couplings between on-shell Z bosons and fermions will be be presented and discussed in the subsequent section on the Z resonance.

4. The vector boson mass interdependence

4.1. One-loop corrections to the muon lifetime

The interdependence between the gauge boson masses is established through the accurately measured muon lifetime or the Fermi coupling constant G_μ, respectively. Originally, the μ-lifetime τ_μ has been calculated within the framework of the effective 4-point Fermi interaction. When QED corrections are included one obtains the result [42]

$$\frac{1}{\tau_\mu} = \frac{G_\mu^2 m_\mu^5}{192\pi^3}\left(1-\frac{8m_e^2}{m_\mu^2}\right)\left[1+\frac{\alpha}{2\pi}(\frac{25}{4}-\pi^2)\right] . \tag{61}$$

The leading $2nd$ order correction is obtained by replacing

$$\alpha \to \alpha\left(1+\frac{2\alpha}{3\pi}\log\frac{m_\mu}{m_e}\right) .$$

This formula is used as the defining equation for G_μ in terms of the experimental μ-lifetime. In lowest order, the Fermi constant is given by the Standard Model expression (26) for the decay amplitude. In 1-loop order, $G_\mu/\sqrt{2}$ coincides with the expression

$$\frac{G_\mu}{\sqrt{2}} = \frac{e_0^2}{8s_W^{0\,2}M_W^{0\,2}}\left[1+\frac{\Sigma^W(0)}{M_W^2}+\delta_{\rm VB}\right] . \tag{62}$$

This equation contains the bare parameters with the bare mixing angle

$$s_W^{0\,2} = 1 - \frac{M_W^{0\,2}}{M_Z^{0\,2}} . \tag{63}$$

The term $\delta_{\rm VB}$ schematically summarizes the vertex corrections and box diagrams in the decay amplitude. A set of infra-red divergent "QED correction" graphs has been

removed from this class of diagrams. These left-out diagrams, together with the real bremsstrahlung contributions, reproduce the QED correction factor of the Fermi model result in Eq. (61) and therefore have no influence on the relation between G_μ and the Standard Model parameters.

Let us evaluate Eq. (62) to 1-loop order by expanding the bare parameters

$$\begin{aligned} e_0^2 &= (e+\delta e)^2 = e^2(1+2\frac{\delta e}{e}), \\ M_W^{0\,2} &= M_W^2\,(1+\frac{\delta M_W^2}{M_W^2}), \\ s_W^{0\,2} &= = s_W^2 + c_W^2\left(\frac{\delta M_Z^2}{M_Z^2}-\frac{\delta M_W^2}{M_W^2}\right) \end{aligned} \tag{64}$$

and keeping only terms of 1-loop order:

$$\begin{aligned} \frac{G_\mu}{\sqrt{2}} &= \frac{e^2}{8 s_W^2 M_W^2}\cdot \\ &\cdot\left[1+2\frac{\delta e}{e}-\frac{c_W^2}{s_W^2}\left(\frac{\delta M_Z^2}{M_Z^2}-\frac{\delta M_W^2}{M_W^2}\right)+\frac{\Sigma^W(0)-\delta M_W^2}{M_W^2}+\delta_{\rm VB}\right] \\ &\equiv \frac{e^2}{8 s_W^2 M_W^2}\cdot[1+\Delta r] \end{aligned} \tag{65}$$

which is the 1-loop version of Eq. (27).

The quantity $\Delta r(e, M_W, M_Z, M_H, m_t)$ is the finite combination of loop diagrams and counterterms in Eq. (65). Since we have already determined the counterterms in the previous subsection in terms of the boson self-energies, it is now only a technical problem to evaluate the 1-loop diagrams for the final explicit expression of Δr. The result is given by

$$\delta_{\rm VB} = \frac{\alpha}{\pi s_W^2}\left(\Delta - \log\frac{M_W^2}{\mu^2}\right) + \frac{\alpha}{4\pi s_W^2}\left(6+\frac{7-4s_W^2}{2s_W^2}\log c_W^2\right). \tag{66}$$

The expression

$$\Delta = \frac{2}{\epsilon} - \gamma + \log 4\pi, \quad \epsilon = 4 - D\,, \tag{67}$$

and the mass scale μ are the conventional UV parameters in dimensional regularization. The singular part of Eq. (66) coincides, up to a factor, with the non-Abelian bosonic contribution to the charge counterterm in Eq. (43):

$$\frac{\alpha}{\pi s_W^2}\left(\Delta - \log\frac{M_W^2}{\mu^2}\right) = \frac{2}{c_W s_W}\frac{\Sigma^{\gamma Z}(0)}{M_Z^2}\,.$$

Together with Eq. (43) and (66) we obtain from Eq. (65):

$$\begin{aligned} \Delta r = \Pi^\gamma(0) &- \frac{c_W^2}{s_W^2}\left(\frac{\delta M_Z^2}{M_Z^2}-\frac{\delta M_W^2}{M_W^2}\right)+\frac{\Sigma^W(0)-\delta M_W^2}{M_W^2} \\ &+2\,\frac{c_W}{s_W}\frac{\Sigma^{\gamma Z}(0)}{M_Z^2} + \frac{\alpha}{4\pi s_W^2}\left(6+\frac{7-4s_W^2}{2s_W^2}\log c_W^2\right). \end{aligned} \tag{68}$$

Via $\Sigma^W(0)$ and the mass counter terms $\delta M^2_{W,Z}$ also the masses M_H, m_t enter Δr, whereas the residual terms depend only on the vector boson masses. The gauge invariant subset of fermion loop corrections has already been discussed in section 3.4. It constitutes the numerically dominating part of Δr. As a result of this discussion, we have got a simple form for Δr in the leading fermionic terms; the full 1-loop expression can be written as follows:

$$\Delta r = \Delta\alpha - \frac{c_W^2}{s_W^2}\,\Delta\rho + (\Delta r)_{\rm rem}\,. \tag{69}$$

$\Delta\alpha$ from Eq. (49) contains the large logarithmic corrections from the light fermions and $\Delta\rho$ from Eq. (54) the leading quadratic correction from the top mass. All other terms are collected in the remainder $(\Delta r)_{\rm rem}$. It should be noted that the remainder also contains a term logarithmic in the top mass (not present in $\Delta\rho$) with a sizeable coefficient:

$$(\Delta r)^{\rm top}_{\rm rem} = -\frac{\alpha}{4\pi s_W^2}\left(\frac{c_W^2}{s_W^2} - \frac{1}{3}\right)\log\frac{m_t}{M_Z} + \cdots \tag{70}$$

Also the Higgs boson contribution is part of the remainder. For large M_H, it increases only logarithmically ("screening" of a heavy Higgs [41]):

$$(\Delta r)^{\rm Higgs}_{\rm rem} \simeq \frac{\alpha}{16\pi s_W^2}\cdot\frac{11}{3}\left(\log\frac{M_H^2}{M_W^2} - \frac{5}{6}\right)\,. \tag{71}$$

The size of $(\Delta r)_{\rm rem}$ is up to ~ 0.01, depending in detail on the value of the Higgs boson mass.

4.2. Higher order contributions

Since Δr contains two large entries, $\Delta\alpha$ and $\Delta\rho$, a careful investigation of higher order effects is necessary.

(i) Summation of large $\Delta\alpha$ terms:

The replacement of the $\Delta\alpha$-part

$$1 + \Delta\alpha \;\to\; \frac{1}{1-\Delta\alpha}$$

of the 1-loop result in Eq. (65) correctly takes into account all orders in the leading logarithmic corrections $(\Delta\alpha)^n$, as can be shown by renormalization group arguments [49]. The evolution of the electromagnetic coupling with the scale μ is described by the renormalization group equation

$$\mu\,\frac{{\rm d}\alpha}{{\rm d}\mu} = -\,\frac{\beta_0}{2\pi}\,\alpha^2 \tag{72}$$

with the coefficient of the 1-loop β-function in QED

$$\beta_0 = -\frac{4}{3}\sum_{f\neq t} Q_f^2\,. \tag{73}$$

The solution of the RGE contains the leading logarithms in the resummed form. It corresponds to a resummation of the iterated 1-loop vacuum polarization to all

orders. The non-leading QED-terms of next order are numerically not significant. Thus, in a situation where large corrections would be due only to the evolution of the electromagnetic charge between two very different scales set by m_f and M_Z, the resummed form

$$G_\mu = \frac{\pi\alpha}{\sqrt{2}M_W^2 s_W^2}\,\frac{1}{1-\Delta r} = \frac{\pi\alpha}{\sqrt{2}M_Z^2 c_W^2 s_W^2}\,\frac{1}{1-\Delta r} \tag{74}$$

with Δr in Eq. (69) would be a reasonable approximation to the full result.

(ii) Summation of large $\Delta\rho$ terms:

For the top quark also $\Delta\rho$ is large and the powers $(\Delta\rho)^n$ are not correctly resummed in Eq. (74). A result correct in the leading terms up to $O(\alpha^2)$ is instead given by the independent resummation [50]

$$\frac{1}{1-\Delta r} \;\to\; \frac{1}{1-\Delta\alpha}\cdot\frac{1}{1+\frac{c_W^2}{s_W^2}\Delta\overline{\rho}} + (\Delta r)_{\rm rem} \tag{75}$$

where

$$\Delta\overline{\rho} = 3x_t[1 + x_t\rho^{(2)}(\frac{M_H}{m_t})], \quad x_t = \frac{G_\mu m_t^2}{8\pi^2\sqrt{2}} \tag{76}$$

incorporates the result from 2-loop 1-particle irreducible diagrams. For light Higgs bosons $M_H \ll m_t$, where M_H can be neglected, the coefficient

$$\rho^{(2)} = 19 - 2\pi^2 \tag{77}$$

was first calculated in ref. [51]. The general function $\rho^{(2)}$, valid for all Higgs masses, has been derived in [52]. With the resummed ρ-parameter

$$\rho = \frac{1}{1-\Delta\overline{\rho}} \tag{78}$$

Eq. (75) is compatible with the following form of the $M_W - M_Z$ interdependence

$$G_\mu \;=\; \frac{\pi}{\sqrt{2}}\,\frac{\alpha(M_Z^2)}{M_W^2\left(1-\frac{M_W^2}{\rho M_Z^2}\right)}\cdot[1+(\Delta r)_{\rm rem}]$$

with $\alpha(M_Z^2)$ given in Eq. (50). It is interesting to compare this result with the corresponding lowest order $M_W - M_Z$ correlation in a more general model with a tree level ρ-parameter $\rho_0 \neq 1$: the tree-level ρ_0 enters in the same way as the ρ from the top-bottom doublet in the minimal model. Wheras in the minimal model ρ is calculable, ρ_0 is an additional free parameter.

(iii) QCD corrections:

Virtual gluons contribute to the quark loops in the vector boson self-energies at the 2-loop level. For the light quarks this QCD correction is already contained in the result for the hadronic vacuum polarization from the dispersion integral, Eq. (47). Fermion loops involving the top quark get additional $O(\alpha\alpha_s)$ corrections which have been calculated perturbatively [53]. The dominating term represents the QCD correction to the leading m_t^2 term of the ρ-parameter and can be built in by writing instead of Eq. (76):

$$\Delta\overline{\rho} = 3x_t\cdot[1 + x_t\,\rho^{(2)} + \delta\rho_{QCD}] \tag{79}$$

The QCD term [54, 55] reads:

$$\delta\rho_{QCD} = -\frac{\alpha_s(\mu)}{\pi}\, c_1 + \left(\frac{\alpha_s(\mu)}{\pi}\right)^2 c_2(\mu) \tag{80}$$

with

$$c_1 = \frac{2}{3}\left(\frac{\pi^2}{3} + 1\right) = 2.8599 \tag{81}$$

and the recently calculated [55] 3-loop coefficent $c_2(\mu)$, which amounts to

$$c_2 = -14.59 \;\text{ for } \mu = m_t \text{ and 6 flavors} \tag{82}$$

with the on-shell top mass m_t. It reduces the scale dependence of ρ significantly and hence is an important entry to decrease the theoretical uncertainty of the standard model predictions for precision observables. As part of the higher order irreducible contributions to ρ, the QCD correction is resummed together with the electroweak 2-loop irreducible term as indicated in Eq. (75).

Beyond the $G_\mu m_t^2 \alpha_s$ approximation through the ρ-parameter, the complete $O(\alpha\alpha_s)$ corrections to the self energies are available from perturbative calculations [53] and by means of dispersion relations [56]. All the higher order terms contribute with the same positive sign to Δr, thus making the top mass dependence of Δr significantly flatter. This is of high importance for the indirect determination of m_t from M_W measurements, which is affected by the order of 10 GeV. Recently, also non-leading terms to Δr of the type

$$\Delta r_{(bt)} = 3x_t \left(\frac{\alpha_s}{\pi}\right)^2 \left(a_1 \frac{M_Z^2}{m_t^2} + a_2 \frac{M_Z^4}{m_t^4}\right)$$

have been computed [57]. They contribute an extra term of $+0.0001$ to Δr and thus are within the uncertainty from $\Delta\alpha$.

(iv) Non-leading electroweak higher order terms:
The modification of Eq. (75) by placing $(\Delta r)_{\rm rem}$ into the denominator

$$\frac{1}{1-\Delta r} \;\to\; \frac{1}{(1-\Delta\alpha)\cdot(1+\frac{c_W^2}{s_W^2}\Delta\overline{\rho}) \;-\; (\Delta r)_{\rm rem}} \tag{83}$$

correctly incorporates the non-leading higher order terms containing mass singularities of the type $\alpha^2 \log(M_Z/m_f)$ [58]

In the meantime, the non-leading higher order electroweak terms of the order $G_\mu^2 m_t^2 M_Z^2$ have been calculated explicitly using the on-shell and the $\overline{MS}$ renormalization schemes [59]. An independent calculaton of the Higgs mass dependence of these 2-loop terms has been performed in ref. [60].

4.3. Predictions and experimental data

The correlation of the electroweak parameters, complete at the one-loop level and with the proper incorporation of the leading higher order effects, is given by the following

equation:

$$M_W^2 \left(1 - \frac{M_W^2}{M_Z^2}\right) = \frac{\pi\alpha}{\sqrt{2}G_\mu} \cdot \frac{1}{(1-\Delta\alpha)\cdot(1+\frac{c_W^2}{s_W^2}\Delta\overline{\rho}) \; - \; (\Delta r)_{\rm rem}}$$
$$\equiv \frac{\pi\alpha}{\sqrt{2}G_\mu} \cdot \frac{1}{1-\Delta r} \, . \tag{84}$$

The term Δr in Eq. (84) is an effective quantity beyond the 1-loop order, introduced to obtain the formal analogy to the naively resummed first order result in Eq. (74). $\Delta\overline{\rho}$ includes the 2-loop irreducible electroweak and QCD corrections to the ρ-parameter according to Eq. (79). The correlation (84) allows us to predict a value for the W mass after the other parameters have been specified. The predicted value for M_W for $m_t = 175.6 \pm 5.5$ GeV is given by

$$M_W \; = \; 80.317^{+0.097}_{-0.098} \pm 0.034 \text{ GeV} \; . \tag{85}$$

The central value is for a Higgs mass of 300 GeV, the upper and lower values belong to $M_H = 70$ and 1000 GeV; the second uncertainty corresponds to the experimental top mass error. The present experimental value for the W mass from the combined UA2, CDF and D0 results [7] is

$$M_W^{exp} \; = \; 80.41 \pm 0.09 \, \text{GeV} \; , \tag{86}$$

and from LEP 2 [6]:

$$M_W^{exp} \; = \; 80.48 \pm 0.14 \, \text{GeV} \; , \tag{87}$$

yielding the average

$$M_W^{exp} \; = \; 80.43 \pm 0.08 \, \text{GeV} \tag{88}$$

in good agreement with the standard model prediction (85).

We can define the higher order quantity Δr also as a physical observable by

$$\Delta r \; = \; 1 \; - \; \frac{\pi\alpha}{\sqrt{2}G_\mu} \, \frac{1}{M_W^2 \left(1 - \frac{M_W^2}{M_Z^2}\right)} \, . \tag{89}$$

Experimentally, it is determined by M_Z and M_W. Theoretically, it can be computed from M_Z, G_μ, α after specifying the masses M_H, m_t by solving Eq. (84). Both electroweak and QCD higher order effects yield a positive shift to Δr and thus diminish the slope of the first order dependence on m_t for large top masses. The effect on Δr coming from the Higgs dependent $\rho^{(2)}$ in Eq. (79) is an additional weakening of the sensitivity to m_t for large Higgs masses.

The theoretical prediction for Δr for various Higgs and top masses is displayed in Figure 1. For comparison with data, the experimental 1σ limits from the direct measurements of $M_Z = 91.1863$ at LEP [6] and M_W, Eq. (88), are indicated. The constraints on the top mass obtained from these results completely coincide with the direct m_t measurement at the Tevatron of $m_t = 175.6 \pm 5.5$ GeV [8]. The present experimental error does not allow a sensitivity to the Higgs mass. Further precision measurements of M_W at LEP 2 will pin down the error to $\delta\Delta r = 0.0024$ The expected precision in the determination of Δr matches the size of $(\Delta r)_{\rm rem}$ and thus will provide some sensitivity also to the Higgs mass.

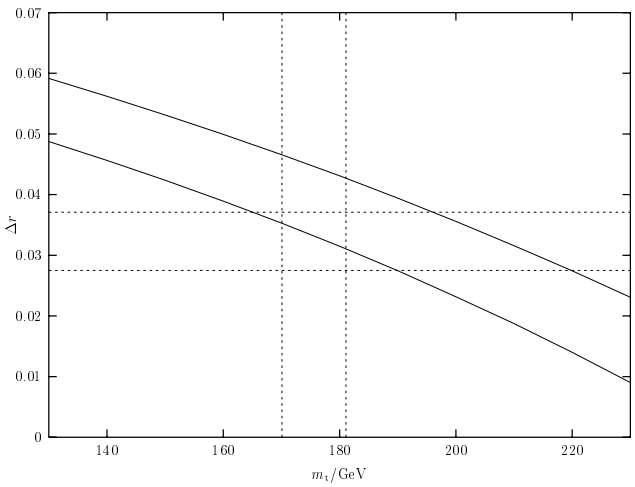

Figure 1. Δr for $M_H = 70$ GeV (lower line) and $M_H = 1$ TeV (upper line), with experimental $\pm 1\sigma$ ranges for m_t and Δr.

4.4. Deep-inelastic neutrino scattering

The quantity s_W^2 resp. the ratio M_W/M_Z can indirectly be measured in the class of low enery experiments comprising neutrino-quark, neutrino-electron, and electron-quark scattering. The two most precise informations come from the NC/CC neutrino-nucleon cross section ratios [61]. For an isoscalar target these ratios do not depend on the nucleon structure [62]:

$$\begin{aligned} R_\nu &= \frac{\sigma_{NC}^\nu}{\sigma_{CC}^\nu} = \left(\frac{M_W}{M_Z}\right)^4 \frac{1 - 2s_W^2 + \frac{10}{9}(1+r)s_W^4}{2(1-s_W^2)^2} \\ R_{\bar\nu} &= \frac{\sigma_{NC}^{\bar\nu}}{\sigma_{CC}^{\bar\nu}} = \left(\frac{M_W}{M_Z}\right)^4 \frac{1 - 2s_W^2 + \frac{10}{9}(1+\frac{1}{r})s_W^4}{2(1-s_W^2)^2} \end{aligned} \tag{90}$$

with $r = \sigma_{CC}^\nu/\sigma_{CC}^{\bar\nu} \simeq 0.4$.

The second factor in R_ν has a very weak dependence on s_W^2. Hence, measurements of R_ν can directly be converted into values for M_W/M_Z. This principal feature remains valid also after the incorporation of radiative corrections in Eq. (90). Besides the QED corrections, vertex corrections and box diagrams which do not depend on m_t, M_H, the dominant effect $\sim m_t^2$ can simply be embedded in Eq. (90) by replacing

$$s_W^2 \to s_W^2 + c_W^2 \Delta\rho \ .$$

This is obvious from the expansion (64) together with Eq. (56). Since an increase in m_t is equivalent to a slight shift in s_W^2, the relation between R_ν and $(M_W/M_Z)^4$ is affected only marginally. This explains qualitatively the stability of M_W/M_Z against variations of m_t when extracted from R_ν.

The present world average on s_W^2 from the experiments CCFR, CDHS and CHARM [61]

$$s_W^2 = 1 - M_W^2/M_Z^2 = 0.2236 \pm 0.0041 \tag{91}$$

corresponds to $M_W = 80.35 \pm 0.21$ GeV and hence is fully consistent with the direct vector boson mass measurements and with the standard theory.

5. The Z resonance in electron-positron annihilation

The measurement of the Z mass from the Z line shape at LEP provides us with an additional precise input parameter besides α and G_μ. Other observable quantities from the Z peak, like total and partial decay widths, asymmetries, τ-polarization, allow us to perform precision tests of the theory by comparison with the theoretical predictions.

5.1. Amplitudes and effective couplings

In lowest order, the processes $e^+e^- \to f\bar{f}$ are described by diagrams with photon and Z exchange (Figure 2). The 1-loop diagrams with virtual photon insertions (virtual QED corrections) form a gauge invariant subset of the full 1-loop terms. The sum of the virtual photon loop graphs is UV finite but IR divergent because of the massless photon. The IR-divergence is cancelled by adding the cross section with real photon bremsstrahlung (after integrating over the phase space for experimentally invisible photons) which always accompanies a realistic scattering process. Since the phase space for invisible photons is a detector dependent quantity the QED corrections cannot in general be separated from the experimental device.

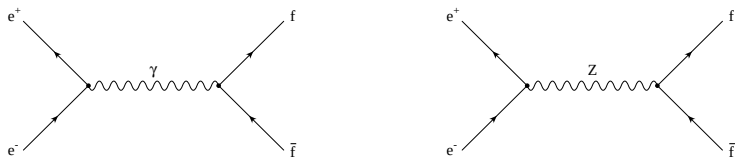

Figure 2. Lowest order photon and Z exchange amplitudes for $e^+e^- \to f\bar{f}$

Our main discussion will focus on the residual set of 1-loop diagrams, the non-QED or weak corrections. This class is free of IR-singularities but sensitive to the details beyond the lowest order amplitudes. The UV-singular terms associated with the loop diagrams are cancelled by our counterterms of section 3 as a consequence of renormalizability. The 1-loop amplitude for $e^+e^- \to f\bar{f}$ contains the sum of the individual contributions to the self-energies and vertex corrections (including the external fermion self-energies via wave function renormalization). The essential steps for getting the total amplitude finite are: expressing the tree diagrams in terms of the bare parameters e_0, $M_Z^{0\,2}$, $s_W^{0\,2}$ expanding the bare quantities according to Eqs. (40,64), and inserting the counterterms given by Eq. (42) and (43). The total amplitude around the Z pole can be cast into a form close to the lowest order amplitude

$$A(e^+e^- \to f\bar{f}) = A_\gamma + A_Z + (box)$$

as the sum of a dressed photon and a dressed Z exchange amplitude plus the contribution from the box diagrams which are numerically not significant around the

peak (relative contribution $< 10^{-4}$). For theoretical consistency (gauge invariance) they have to be retained; for practical purposes they can be neglected in Z physics. Resummation of the iterated self-energy insertions in the photon and Z propagators brings the finite Z decay width into the denominator, and treats the higher order leading terms in the proper way. Since the leading terms arise from fermion loops only, we do not have problems with gauge invariance; the bosonic loop terms have to be understood as expanded to strict 1-loop order. Numerically their resummation does not yield significant differences but allows a simple and compact notation.

Dressed photon amplitude:

The dressed photon exchange amplitude, with $(p_{e^+} + p_{e^-})^2$,

$$A_\gamma = \frac{e^2}{1+\hat{\Pi}^\gamma(s)} \cdot \frac{Q_e Q_f}{s} \cdot \\ \cdot [(1+F_V^{\gamma e})\gamma_\mu - F_A^{\gamma e}\gamma_\mu\gamma_5] \otimes [(1+F_V^{\gamma f})\gamma^\mu - F_A^{\gamma f}\gamma^\mu\gamma_5] \tag{92}$$

contains $\hat{\Pi}^\gamma$ as the γ self-energy subtracted at $s = 0$. Writing it in the denominator takes into account the resummation of the leading log's from the light fermions, around the Z given by

$$\hat{\Pi}^\gamma_{\rm ferm}(s) = -0.0593 - \frac{40\alpha}{18\pi}\log\frac{s}{M_Z^2} \pm 0.0007 + \mathrm{i}\,\frac{\alpha}{3}\sum_{f\neq t} Q_f^2 N_C^f\,. \tag{93}$$

The form factors $F_{V,A}(s)$ arise from the vertex correction diagrams together with the external fermion self-energies. They vanish for real photons: $F_{V,A}^{\gamma e,f}(0) = 0$. The typical size of the various corrections is (real parts):

$$\hat{\Pi}^\gamma(M_Z^2) = -0.06 \\ F_V^{\gamma e}(M_Z^2) \simeq F_A^{\gamma e}(M_Z^2) \simeq 10^{-3}\,.$$

For the region around the Z peak, the vertex form factors are thus negligible.

Dressed Z amplitude:

Without the box diagrams the corrections factorize and we obtain a result quite close to the Born amplitude:

$$A_Z = \sqrt{2}G_\mu M_Z^2(\rho_e\rho_f)^{1/2} \cdot \\ \cdot \frac{[\gamma_\mu(I_3^e - 2Q_e s_W^2\kappa_e) - I_3^e\gamma_\mu\gamma_5] \otimes [\gamma^\mu(I_3^f - 2Q_f s_W^2\kappa_f) - I_3^f\gamma^\mu\gamma_5]}{s - M_Z^2 + \mathrm{i}\,\frac{s}{M_Z^2}\cdot M_Z\Gamma_Z}\,. \tag{94}$$

The weak corrections appear in terms of fermion-dependent form factors ρ and κ in the coupling constants and in the width in the denominator.

The s-dependence of the imaginary part is due to the s-dependence of $\mathrm{Im}\Sigma^Z$; the linearization is completely sufficient in the resonance region. We postpone the discussion of the Z width for the moment and continue with the form factors.

The form factors ρ and κ in Eq. (94 have universal parts (i.e. independent of the fermion species) and non-universal parts which explicitly depend on the type of the external fermions. The universal parts arise from the counterterms and the boson

self-energies, the non-universal parts from the vertex corrections and the fermion self-energies in the external lines. In their leading terms the universal contributions have already been discussed in section 3.4. For incorporating the next order leading terms one has to perform the substitutions .

$$\begin{aligned}
\rho_{e,f} &= 1 + \Delta\rho + \cdots \qquad \to \frac{1}{1-\Delta\overline{\rho}} + \cdots \\
\kappa_{e,f} &= 1 + \frac{c_W^2}{s_W}\Delta\rho + \cdots \to 1 + \frac{c_W^2}{s_W}\Delta\overline{\rho} + \cdots
\end{aligned} \tag{95}$$

with $\Delta\overline{\rho}$ from Eq. (79).

Neutral current effective couplings:

The factorized Z amplitude allows us to define NC vertices at the Z resonance with effective coupling constants $g^f_{V,A}$, synonymously to the use of ρ_f, κ_f:

$$\begin{aligned}
\Gamma^{\rm NC}_\mu &= \left(\sqrt{2}G_\mu M_Z^2 \rho_f\right)^{1/2} \left[(I_3^f - 2Q_f s_W^2 \kappa_f)\gamma_\mu - I_3^f \gamma_\mu\gamma_5\right] \\
&= \left(\sqrt{2}G_\mu M_Z^2\right)^{1/2} \left[g_V^f\,\gamma_\mu - g_A^f\,\gamma_\mu\gamma_5\right].
\end{aligned} \tag{96}$$

The complete expressions for the effective couplings read as follows:

$$\begin{aligned}
g_V^f &= \left[v_f + 2 s_W c_W\, Q_f \frac{\hat\Pi^{\gamma Z}(M_Z^2)}{1+\hat\Pi^\gamma(M_Z^2)} + F_V^{Zf}\right] \left(\frac{1-\Delta r}{1+\hat\Pi^Z(M_Z^2)}\right)^{1/2}, \\
g_A^f &= \left[a_f + F_A^{Zf}\right] \left(\frac{1-\Delta r}{1+\hat\Pi^Z(M_Z^2)}\right)^{1/2}.
\end{aligned} \tag{97}$$

Besides Δr, the building blocks, are the following finite combinations of 2-point functions evaluated at $s = M_Z^2$:

$$\begin{aligned}
\hat\Pi^Z(s) &= \frac{{\rm Re}\,\Sigma^Z(s) - \delta M_Z^2}{s - M_Z^2} - \Pi^\gamma(0) \\
&\quad + \frac{c_W^2 - s_W^2}{s_W^2}\left(\frac{\delta M_Z^2}{M_Z^2} - \frac{\delta M_W^2}{M_W^2} - 2\,\frac{s_W}{c_W}\,\frac{\Sigma^{\gamma Z}(0)}{M_Z^2}\right), \\
\hat\Pi^{\gamma Z}(s) &= \frac{\Sigma^{\gamma Z}(s) - \Sigma^{\gamma Z}(0)}{s} - \frac{c_W}{s_W}\left(\frac{\delta M_Z^2}{M_Z^2} - \frac{\delta M_W^2}{M_W^2}\right) + 2\,\frac{\Sigma^{\gamma Z}(0)}{M_Z^2}
\end{aligned} \tag{98}$$

and the finite form factors $F_{V,A}$ at $s = M_Z^2$ from the vertex corrections (includng with the external fermion wave function renormalizations)

$$\begin{aligned}
&\Delta\Gamma^{\rm Z}_\mu = \\
&\frac{e}{2 s_W c_W}\left\{\gamma_\mu F_V^{Zf}(s) - \gamma_\mu\gamma_5 F_A^{Zf}(s) + I_3^f \gamma_\mu(1-\gamma_5)\cdot\frac{c_W}{s_W}\,\frac{\Sigma^{\gamma Z}(0)}{M_Z^2}\right\},
\end{aligned}$$

Due to the imaginary parts of the self energies and vertices, the form factors and the effective couplings, respectively, are complex quantities. For the explicit expressions see [26].

The Zbb couplings:

For the light fermions ($f \neq b, t$) the non-universal contributions are small, and (practically) independent of m_t, M_H which enter only the universal part. This is, however, not true for the b-quark where also the non-universal parts have a strong dependence on m_t [63] resulting from the virtual top quark in the vertex corrections. The difference between the d and b couplings can be parametrized in the following way

$$\rho_b = \rho_d (1+\tau)^2, \quad s_b^2 = s_d^2 (1+\tau)^{-1} \tag{99}$$

with the quantity

$$\tau = \Delta\tau^{(1)} + \Delta\tau^{(2)} + \Delta\tau^{(\alpha_s)}$$

calculated perturbatively, at the present level comprising: the complete 1-loop order term [63] with x_t from Eq. (76):

$$\Delta\tau^{(1)} = -2x_t - \frac{G_\mu M_Z^2}{6\pi^2\sqrt{2}}(c_W^2+1)\log\frac{m_t}{M_W} + \cdots, \tag{100}$$

the leading electroweak 2-loop contribution of $O(G_\mu^2 m_t^4)$ [52, 64]

$$\Delta\tau^{(2)} = -2\, x_t^2\, \tau^{(2)}\,, \tag{101}$$

where $\tau^{(2)}$ is a function of M_H/m_t with $\tau^{(2)} = 9 - \pi^2/3$ for $M_H \ll m_t$; the QCD corrections to the leading term of $O(\alpha_s G_\mu m_t^2)$ [65]

$$\Delta\tau^{(\alpha_s)} = 2\, x_t \cdot \frac{\alpha_s}{\pi} \cdot \frac{\pi^2}{3}\,, \tag{102}$$

and the $O(\alpha_s)$ correction to the $\log m_t/M_W$ term in (100), with a numerically very small coefficient [66].

Effective mixing angles:

Due to the imaginary parts of the self energies and vertices, the form factors and the effective couplings, respectively, are complex quantities. We can define effective mixing angles according to

$$s_f^2 := \sin^2\theta_f = s_W^2\, \mathrm{Re}\,\kappa_f = \frac{1}{4\mid Q_f \mid}\left(1 - \frac{\mathrm{Re}\, g_V^f}{\mathrm{Re}\, g_A^f}\right). \tag{103}$$

from the effective coupling constants in (97). They are of particular interest since they determine the on-resonance asymmetries, which will be discussed later in section 5.4. Figure 3 displays the leptonic mixing angle s_e^2 and its compatibility with the data.

5.2. The Z line shape

The integrated cross section $\sigma(s)$ for $e^+e^- \to f\bar{f}$ around the Z resonance with unpolarized beams is obtained from the formulae of the previous section in a straight forward way, expressed in terms of the effective vector and axial vector coupling constants. It is, however, convenient to rewrite $\sigma(s)$ in terms of the Z width and the partial widths Γ_e, Γ_f in order to have a more model independent parametrization.

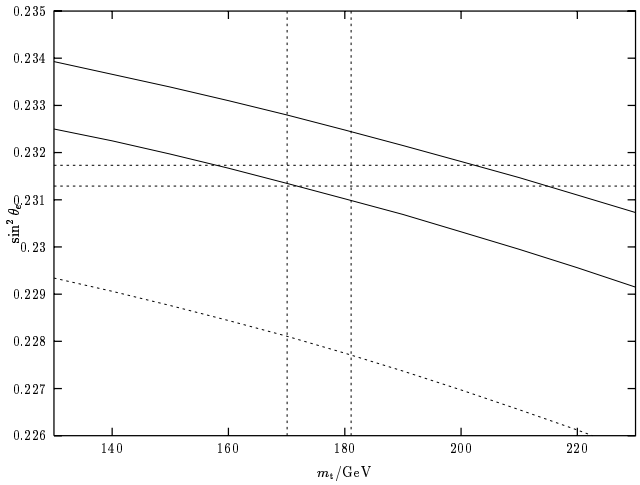

Figure 3. $\sin^2\theta_e$ for $M_H = 70$ GeV (lower line) and $M_H = 1$ TeV (upper line). Also shown are the experimental data ($\pm 1\sigma$ ranges) for m_t and s_e^2 (LEP/SLC average). The dotted curve includes only the fermionic loop effects via $\Delta\alpha$ and $\Delta\rho$.

The following form [67, 68] includes final state photon radiation, Eq. (115), and QCD corrections in case of quark final states, Eq. (117): †

$$\sigma(s) = \frac{12\pi\Gamma_e\Gamma_f}{\mid s - M_Z^2 + iM_Z\Gamma_Z(s) \mid^2}\left\{\frac{s}{M_Z^2} + R_f\,\frac{s-M_Z^2}{M_Z^2} + I_f\,\frac{\Gamma_Z}{M_Z} + \cdots\right\}$$
$$+\ \frac{4\pi\,\alpha(s)^2}{3s}\,Q_f^2 N_C^f\,K_{\rm QCD}\,(1+\delta_{\rm QED}) \qquad (104)$$

with

$$\Gamma_Z(s) = \Gamma_Z\left\{\frac{s}{M_Z^2} + \epsilon\,\frac{s-M_Z^2}{M_Z^2} + \cdots\right\} \qquad (105)$$

and $N_C^f = 1$ for leptons and $= 3$ for quarks. The terms R_f, I_f, ϵ are small quantities calculable in terms of the basic parameters. R_f and I_f describe the γ-Z interference (improved Born approximation)

$$R_f = \frac{2\,Q_e Q_f g_V^e g_V^f}{[(g_V^e)^2+(g_A^e)^2][(g_V^f)^2+(g_A^f)^2]}\,\frac{4\pi\alpha(s)}{\sqrt{2}G_\mu M_Z^2}$$
$$I_f\ = \frac{2\,Q_e Q_f g_V^e g_V^f}{[(g_V^e)^2+(g_A^e)^2][(g_V^f)^2+(g_A^f)^2]}\,\frac{4\pi\alpha(s)}{\sqrt{2}G_\mu M_Z^2}\cdot\frac{s}{M_Z^2}\,{\rm Im}\,\hat{\Pi}^\gamma\,, \qquad (106)$$

and the last term is the QED background from pure photon exchange with

$$\alpha(s) = \frac{\alpha}{1 + {\rm Re}\,\hat{\Pi}^\gamma_{\rm ferm}(s)}$$

† Since initial state photon radiation is treated separately the QED correction factor in Eq. (104) has to be removed in Γ_e.

and $\hat{\Pi}^{\gamma}_{\rm ferm}$ from Eq. (93). The small correction

$$\epsilon = \sum_f \epsilon_f, \quad \epsilon_f \simeq \frac{6m_f^2}{M_Z^2}\frac{\Gamma_f}{\Gamma_Z}\frac{(g_A^f)^2}{(g_V^f)^2+(g_A^f)^2}$$

is due to finite fermion mass effects in the final states. I_f and ϵ have negligible influence on the line shape.

The s-dependent width gives rise to a dislocation of the peak maximum by $\simeq -34$ MeV [69, 70]. The first term in the expansion (104) is the pure Z resonance. It differs from a Breit-Wigner shape by the s-dependence of the width:

$$\sigma_{\rm res}(s) = \sigma_0 \frac{s\Gamma_Z^2}{(s-M_Z^2)^2+s^2\Gamma_Z^2/M_Z^2}, \quad \sigma_0 = \frac{12\pi}{M_Z^2}\cdot\frac{\Gamma_e\Gamma_f}{\Gamma_Z^2}\,. \tag{107}$$

By means of the substitution [70]

$$s - M_Z^2 + is\Gamma_Z/M_Z = (1+i\gamma)(s-\hat{M}_Z^2+i\hat{M}_Z\hat{\Gamma}_Z) \tag{108}$$

with

$$\hat{M}_Z = M_Z(1+\gamma^2)^{-1/2}, \;\; \hat{\Gamma}_Z = \Gamma_Z(1+\gamma^2)^{-1/2}, \;\; \gamma = \frac{\Gamma_Z}{M_Z} \tag{109}$$

a Breit-Wigner resonance shape is recovered:

$$\sigma_{\rm res}(s) = \sigma_0 \frac{s\hat{\Gamma}_Z^2}{(s-\hat{M}_Z^2)^2+\hat{M}_Z^2\hat{\Gamma}_Z^2} \tag{110}$$

Numerically one finds: $\hat{M}_Z - M_Z \simeq -34$ MeV, $\hat{\Gamma}_Z - \Gamma_Z \simeq -1$ MeV. σ_0 is not changed. $\hat{M}_Z$ corresponds to the real part of the S-matrix pole of the Z-resonance [37].

QED corrections:

The observed cross section is the result of convoluting Eq. (104) with the initial state QED corrections consisting of virtual photon and real photon bremsstrahlung contributions:

$$\sigma_{\rm obs}(s) = \int_0^{k_{\rm max}} dk\, H(k)\, \sigma(s(1-k))\,. \tag{111}$$

$k_{\rm max}$ denotes a cut to the radiated energy. Kinematically it is limited by $1-4m_f^2/s$ or $1-4m_\pi^2/s$ for hadrons, respectively. For the required accuracy, multi-photon radiation has to be included. The radiator function $H(k)$ with soft-photon resummation and the exact $O(\alpha^2)$ result [71] for initial state QED corrections is given in ref. [67]

From line shape measurements one obtains the parameters M_Z, Γ_Z, σ_0 or the partial widths, respectively. Whereas M_Z is used as a precise input parameter, together with α and G_μ, the width and partial widths allow comparisons with the predictions of the Standard Model to be discussed next.

5.3. Z widths and partial widths

The total Z width Γ_Z can be calculated as the sum over the partial decay widths

$$\Gamma_Z = \sum_f \Gamma_f + \cdots, \quad \Gamma_f = \Gamma(Z\to f\bar{f})\,, \tag{112}$$

Other decay modes are not significant. The fermionic partial widths, when expressed in terms of the effective coupling constants defined in Eq. (97), read:

$$\Gamma_f = \Gamma_0 \sqrt{1-\frac{4m_f^2}{M_Z^2}} \left[\mid g_V^f \mid^2 \left(1+\frac{2m_f^2}{M_Z^2}\right) + \mid g_A^f \mid^2 \left(1-\frac{4m_f^2}{M_Z^2}\right)\right] \cdot$$
$$\cdot \; (1+\delta_{\rm QED}) \; + \; \Delta\Gamma^f_{\rm QCD} \qquad (113)$$
$$\simeq \Gamma_0 \left[\mid g_V^f \mid^2 + \mid g_A^f \mid^2 \left(1-\frac{6m_f^2}{M_Z^2}\right)\right] \cdot (1+\delta_{\rm QED}) \; + \; \Delta\Gamma^f_{\rm QCD}$$

with

$$\Gamma_0 \; = \; N_C^f \, \frac{\sqrt{2} G_\mu M_Z^3}{12\pi} \, . \qquad (114)$$

The photonic QED correction

$$\delta_{\rm QED} = Q_f^2 \, \frac{3\alpha}{4\pi} \qquad (115)$$

is very small, maximum 0.17% for charged leptons.

The factorizable QCD corrections for hadronic final states can be written as follows:

$$\Delta\Gamma^f_{\rm QCD} \; = \; \Gamma_0 \left[\mid g_V^f \mid^2 + \mid g_A^f \mid^2 \right] \cdot K_{\rm QCD} \qquad (116)$$

with [72]

$$K_{\rm QCD} = \frac{\alpha_s}{\pi} + 1.41 \left(\frac{\alpha_s}{\pi}\right)^2 - 12.8 \left(\frac{\alpha_s}{\pi}\right)^3 - \frac{Q_f^2}{4} \frac{\alpha\alpha_s}{\pi^2} \qquad (117)$$

for the light quarks with $m_q \simeq 0$. The recently obtained non-factorizable part of the 2-loop $O(\alpha\alpha_s)$ QCD corrections [73] yields an extra negtive contribution to the partial widths of

$$-1.24(4) \times 10^{-4} {\rm GeV} \quad (u\bar{u})$$
$$-1.73(6) \times 10^{-4} {\rm GeV} \quad (d\bar{d}) \, ,$$

and -0.59(3) MeV for the total hadronic Z width Γ_{had}, respectively.

For b quarks the QCD corrections are different due to finite b mass terms and to top quark dependent 2-loop diagrams for the axial part [74]:

$$\Delta\Gamma^b_{\rm QCD} = \Gamma_0 \left[\mid g_V^b \mid^2 + \mid g_A^b \mid^2 \right] \cdot K_{\rm QCD}$$
$$+ \Gamma_0 \mid g_V^b \mid^2 \cdot \frac{12 m_b^2}{M_Z^2} \left[\frac{\alpha_s}{\pi} + \left(\frac{\alpha_s}{\pi}\right)^2 (6.07 - 2\ell) \right.$$
$$\left. + \left(\frac{\alpha_s}{\pi}\right)^3 (2.38 - 24.29\ell + 0.083\ell^2) \right]$$
$$+ \Gamma_0 \mid g_A^b \mid^2 \cdot \frac{6 m_b^2}{M_Z^2} \left[\frac{\alpha_s}{\pi} (2\ell - 1) + \left(\frac{\alpha_s}{\pi}\right)^2 (17.96 + 14.14\ell - 0.083\ell^2) \right]$$
$$+ \Gamma_0 \mid g_A^b \mid^2 \cdot \frac{1}{3} \left(\frac{\alpha_s}{\pi}\right)^2 I(M_Z^2/4m_t^2) \qquad (118)$$

with

$$\ell = \log \frac{M_Z^2}{m_b^2}$$

and [75]

$$I(x) \simeq -9.250 + 1.037x + 0.632x^2 + 6\,\log(2\sqrt{x})\,.$$

Radiation of secondary fermions through photons from the primary final state fermions can yield another sizeable contribution to the partial Z widths which, however, is compensated by the corresponding virtual contribution through the dressed photon propagator in the final state vertex correction. For this compensation it is essential that the analysis is inclusive enough, i.e. the cut to the invariant mass of the secondary fermions is sufficiently large [76].

In table 1 the Standard Model predictions for the various partial widths and the total width of the Z boson are collected. They include all the electroweak, QED and QCD corrections discussed above. Of particular interest are the following ratios of partial widths

$$R_{had} = \frac{\Gamma_{had}}{\Gamma_e}, \quad R_b = \frac{\Gamma_b}{\Gamma_{had}}, \quad R_c = \frac{\Gamma_c}{\Gamma_{had}}. \tag{119}$$

R_{had} is most sensitive to α_s, R_b to the top mass m_t, and R_c shows very little variation with the standard model input parameters (see also table 5).

Table 1. Partial and total Z widths in MeV for $m_t = 175$ GeV and various Higgs masses (in GeV). $\alpha_s = 0.118$. Not listed are the values for $\Gamma_\tau = 0.9977\,\Gamma_e$ and Γ_c (very close to Γ_u).

M_H	Γ_ν	Γ_e	Γ_u	Γ_d	Γ_b	Γ_{had}	Γ_{tot}	R_{had}
60	167.3	84.06	300.5	383.3	375.9	1743.5	2497.3	20.74
300	167.2	83.95	299.8	382.5	375.2	1740.0	2493.1	20.72
1000	166.9	83.81	299.0	381.7	374.2	1736.0	2488.0	20.71

5.4. Asymmetries

5.4.1. Left-right asymmetry: The left-right asymmetry is defined as the ratio

$$A_{\rm LR} = \frac{\sigma_L - \sigma_R}{\sigma_L + \sigma_R} \tag{120}$$

where $\sigma_{L(R)}$ denotes the integrated cross section for left (right) handed electrons. $A_{\rm LR}$, in case of lepton universality, is equal to the final state polarization in τ-pair production:

$$A_{pol}^\tau = A_{\rm LR}\,. \tag{121}$$

The on-resonance asymmetry ($s = M_Z^2$) is given by

$$A_{\rm LR}(M_Z^2) = A_e \;+\; \Delta A_{\rm LR}^I \;+\; \Delta A_{\rm LR}^Q \tag{122}$$

where the combination (here we neglect the small imaginary parts of the couplings)

$$A_e = \frac{2g_V^e g_A^e}{(g_V^e)^2 + (g_A^e)^2} = \frac{2(1-4\sin^2\theta_e)}{1+(1-4\sin^2\theta_e)^2} \tag{123}$$

depends only on the effective mixing angle Eq. (103) for the electron. The small contributions from the interference with the photon exchange

$$\Delta A_{\rm LR}^I = \frac{2Q_e Q_f\, g_A^e g_V^f}{(g_V^{e\,2} + g_A^{e\,2})\,(g_V^{f\,2} + g_A^{f\,2})} \frac{4\pi\alpha(M_Z^2)}{\sqrt{2}G_\mu M_Z^2} \cdot \frac{\Gamma_Z}{M_Z} \cdot {\rm Im}\,\hat{\Pi}^\gamma \tag{124}$$

and from the pure photon exchange part

$$\Delta A_{\rm LR}^Q = -\frac{A_e\, Q_e^2 Q_f^2}{(g_V^{e\,2} + g_A^{e\,2})\,(g_V^{f\,2} + g_A^{f\,2})} \left(\frac{4\pi\alpha(M_Z^2)}{\sqrt{2}G_\mu M_Z^2}\right)^2 \left(\frac{\Gamma_Z}{M_Z}\right)^2 . \tag{125}$$

are listed in table 2 for the various final state fermions. Except from lepton final states, they are negligibly small. Mass effects from final fermions practically cancel. The same holds for QCD corrections in the case of quark final states, final state QED corrections, and QED corrections from the interference of initial-final state photon radiation. Initial state QED corrections can be treated in complete analogy to Eq. (111) applied to $\sigma_{L,R}(s)$. Their net effect in the asymmetry is also very small and practically independent of cuts [77, 78]. $A_{\rm LR}$ thus represents a unique laboratory for testing the non-QED part of the electroweak theory. Measurements of $A_{\rm LR}$ are essentially measurements of $\sin^2\theta_e$ or of the ratio g_V^e/g_A^e.

Table 2. Contributions to the on-resonance left-right asymmetry for various final state fermions. $\sin^2\theta_e = 0.2315$.

f	A_e	$\Delta A_{\rm LR}^I$	$\Delta A_{\rm LR}^Q$
μ	0.1511	0.0002	-0.0009
τ	0.1511	0.0002	-0.0009
c	0.1511	0.0005	-0.0003
b	0.1511	0.0004	-0.0001

5.4.2. Forward-backward asymmetries: The forward-backward asymmetry is defined by

$$A_{\rm FB} = \frac{\sigma_F - \sigma_B}{\sigma_F + \sigma_B} \tag{126}$$

with

$$\sigma_F = \int_{\theta>\pi/2} d\Omega\, \frac{d\sigma}{d\Omega}\,, \quad \sigma_B = \int_{\theta<\pi/2} d\Omega\, \frac{d\sigma}{d\Omega}\,. \tag{127}$$

For the on-resonance asymmetry ($s = M_Z^2$) we obtain

$$A_{\rm FB}(M_Z^2) = \frac{3}{4} \cdot A_e\, A_f \left(1 - 4\mu_f + 6\mu_f \frac{(g_A^f)^2}{(g_V^f)^2 + (g_A^f)^2}\right) + \Delta A_{\rm FB}^I + \Delta A_{\rm FB}^Q\,. \tag{128}$$

A_f is defined as

$$A_f \;=\; \frac{2g_V^f g_A^f}{(g_V^f)^2+(g_A^f)^2} \;=\; \frac{2(1-4\mid Q_f\mid s_f^2)}{1+(1-4\mid Q_f\mid s_f^2)^2}\,. \tag{129}$$

The small contributions $\Delta A_{\rm FB}^{I,Q}$ result from the the interference with the photon exchange

$$\Delta A_{\rm FB}^{I} = \frac{3}{4}\,\frac{2Q_eQ_f\,g_A^e g_A^f}{(g_V^{e\,2}+g_A^{e\,2})\,(g_V^{f\,2}+g_A^{f\,2})}\,\frac{4\pi\alpha(M_Z^2)}{\sqrt{2}G_\mu M_Z^2}\cdot\frac{\Gamma_Z}{M_Z}\cdot{\rm Im}\,\hat{\Pi}^\gamma \tag{130}$$

and from the pure photon exchange part:

$$\Delta A_{\rm FB}^{Q} \;=\; -\;\frac{3}{4}\,\frac{A_eA_f\,Q_e^2Q_f^2}{(g_V^{e\,2}+g_A^{e\,2})\,(g_V^{f\,2}+g_A^{f\,2})}\left(\frac{4\pi\alpha(M_Z^2)}{\sqrt{2}G_\mu M_Z^2}\right)^2\left(\frac{\Gamma_Z}{M_Z}\right)^2\,. \tag{131}$$

QED corrections to the forward-backward asymmetries are summarized in [79]. The on-resonance asymmetries are essentially determined by the values of the effective mixing angles for e and f entering the product A_eA_f. Through $s_{e,f}^2$ also the dependence of the asymmetries on the basic Standard Model parameters m_t, M_H is fixed. The small corrections from finite mass effects, interference and photon exchange can be considered practically independent of the details of the model. For demonstrational purpose we list in table 3 the various terms in the on-resonance asymmetries according to Eq. (128) for a common value of the effective mixing angle $s_e^2 = s_f^2 = 0.2315$.

Table 3. On-resonance forward-backward asymmetries for $s_f^2 = 0.2315$.

f	$\frac{3}{4}A_eA_f$	mass correction	$\Delta A_{\rm FB}^I$	$\Delta A_{\rm FB}^Q$
μ	0.0171	$< 10^{-6}$	0.0018	-0.0001
τ	0.0171	$1.3\cdot10^{-5}$	0.0018	-0.0001
c	0.0758	$2.5\cdot10^{-5}$	0.0011	-0.0002
b	0.1061	$1.5\cdot10^{-5}$	0.0004	$-5\cdot10^{-5}$

5.5. Uncertainties of the Standard Model predictions

In order to establish in a significant manner possibly small effects from unknown physics we have to know the uncertainties of our theoretical predictions which have to be confronted with the experiments.

The sources of uncertainties in theoretical predictions are the following:

- the experimental errors of the parameters used as an input. With the choice α, G_μ, and M_Z from LEP we can keep these errors as small as possible. The errors from this source are then determined by δM_Z since the errors of α and G_μ are negligibly small. For any of the mixing angles s_W^2, s_f^2 one finds

$$\frac{\delta s^2}{s^2} = \frac{2\,c^2}{c^2-s^2}\,\frac{\delta M_Z}{M_Z} \;\simeq 2\cdot10^{-5}\,. \tag{132}$$

- the uncertainties from quark loop contributions to the radiative corrections . Here, we have to distinguish two cases: the uncertainties from the light quark contributions to $\Delta\alpha$ and the uncertainties from the heavy quark contributions to $\Delta\rho$. In both cases the uncertainties are due to strong interaction effects, which are not sufficiently under control theoretically. The problems are due to:
  (i) the QCD parameters. The scale of α_s and the definition and scale of quark masses to be used in the calculation of a particular quantity are quite ambiguous in many cases.
  (ii) the bad convergence and/or breakdown of perturbative QCD. In particular at low q^2 and in the resonance regions theoretically poorly known nonperturbative effects are non-negligible.
  The theoretical problems with the hadronic contributions of the 5 light quarks to $\Delta\alpha$ is circumvented by using the experimental e^+e^--annihilation cross-section $\sigma(e^+e^- \to \gamma^* \to \text{hadrons})$. The error [43]
  $$\delta(\Delta\alpha) = \pm 0.0007$$
  is dominated by the large experimental errors in $\sigma_{tot}(e^+e^- \to \gamma^* \to \textit{hadrons})$ and can be improved only by more precise measurements of hadron production in e^+e^--annihilation at energies well below M_Z. The present uncertainty leads to an error in the W-mass prediction
  $$\frac{\delta M_W}{M_W} = \frac{s_W^2}{c_W^2 - s_W^2}\frac{\delta(\Delta r)}{2(1-\Delta r)}$$
  of $\delta M_W = 13$ MeV and $\delta \sin^2\theta = 0.00023$ in the prediction of the various weak mixing parameters s_W^2, s_f^2. This matches with the present experimental precision in the electroweak mixing angle.
- The uncertainties from the QCD contributions, besides the 1.6 MeV in the hadronic Z width from $\delta\alpha_s = 0.003$, can essentially be traced back to those in the top quark loops for the ρ-parameter. They can be combined into the following errors [80], which have improved due to the recently available 3-loop result:
  $$\delta(\Delta\rho) \simeq 1.5 \cdot 10^{-4},\ \delta s_\ell^2 \simeq 0.0001$$
  for $m_t = 175$ GeV.
- the uncertainties from omission of higher order effects. The size of unknown higher order contributions can be estimated by different treatments of non-leading terms of higher order in the implementation of radiative corrections in electroweak observables ('options') and by investigations of the scheme dependence. Explicit comparisons between the results of 5 different computer codes based on on-shell and $\overline{MS}$ calculations for the Z resonance observables are documented in the "Electroweak Working Group Report" [81] in ref. [9]. Table 4 shows the uncertainty in a selected set of precision observables. The recently calculated non-leading 2-loop corrections [59] $\sim G_\mu^2 m_t^2 M_Z^2$ for Δr and s_ℓ^2 are not included in table 4. It is expected that they reduce the uncertainty in M_W and s_ℓ^2 considerably, by at least a factor ~ 0.5.

6. Theory and precision data

6.1. Standard model predictions

In this section we put together the standard model predictions for the discussed set of precision observables for comparison with the most recent experimental data. The

Table 4. Largest half-differences among central values (Δ_c) and among maximal and minimal predictions (Δ_g) for $m_t = 175\,\mathrm{GeV}$, $60\,\mathrm{GeV} < M_H < 1\,\mathrm{TeV}$ (from ref. [81])

Observable O	$\Delta_c O$	$\Delta_g O$
M_W (GeV)	4.5×10^{-3}	1.6×10^{-2}
Γ_e (MeV)	1.3×10^{-2}	3.1×10^{-2}
Γ_Z (MeV)	0.2	1.4
s_e^2	5.5×10^{-5}	1.4×10^{-4}
s_b^2	5.0×10^{-5}	1.5×10^{-4}
R_{had}	4.0×10^{-3}	9.0×10^{-3}
R_b	6.5×10^{-5}	1.7×10^{-4}
R_c	2.0×10^{-5}	4.5×10^{-5}
σ_0^{had} (nb)	7.0×10^{-3}	8.5×10^{-3}
A_{FB}^l	9.3×10^{-5}	2.2×10^{-4}
A_{FB}^b	3.0×10^{-4}	7.4×10^{-4}
A_{FB}^c	2.3×10^{-4}	5.7×10^{-4}
A_{LR}	4.2×10^{-4}	8.7×10^{-4}

values for the various forward-backward asymmetries are for the pure resonance term only. The small photon and interference contributions in Eq. (128) are subtracted from the data, as well as the QED corrections. In table 5 the Standard Model predictions for Z pole observables and the W mass are put together for a light and a heavy Higgs particle with $m_t = 175$ GeV. The last column is the variation of the prediction according to $\Delta m_t = \pm 6$ GeV. The input value for α_s is chosen as $\alpha_s = 0.118$ [82]. Not included are the uncertainties from $\delta\alpha_s = 0.003$, which amount to 1.6 MeV for the hadronic Z width, 0.038 nb for the hadronic peak cross section, and 0.019 for R_{had}. The other observables are insensitive to small variations of α_s. The experimental results on the Z observables are from LEP and SLD (A_b, A_c and s_e^2 from A_{LR}). The leptonic mixing angle determined via A_{LR} by SLD and the s_ℓ^2 average from LEP differ by about 3 standard deviations:

$$s_e^2(A_{\mathrm{LR}}) = 0.23055 \pm 0.00041$$
$$s_\ell^2(\mathrm{LEP}) = 0.23196 \pm 0.00027\,.$$

The table contains the combine LEP/SLD value. ρ_ℓ and s_ℓ^2 are the leptonic neutral current couplings in eq. (96), derived from partial widths and asymmetries under the assumption of lepton universality. The table illustrates the sensitivity of the various quantities to the Higgs mass. The effective mixing angle turns out to be the most sensitive observable, where both the experimental error and the uncertainty from m_t are small compared to the variation with M_H. Since a light Higgs boson corresponds to a low value of s_ℓ^2, the strongest upper bound on M_H is from A_{LR} at the SLC [83], whereas LEP data alone allow to accommodate also a relatively heavy Higgs (see figure 5). Further constraints on M_H are to be expected in the future from more precise M_W measurements at LEP 2 and the upgraded Tevatron.

Note that the experimental value for ρ_ℓ points out the presence of genuine

Table 5. Precision observables: experimental results [6] and standard model predictions.

observable	exp.	$M_H = 65$ GeV	$M_H = 1$ TeV	Δm_t
M_Z (GeV)	91.1863 ± 0.0019	input	input	
Γ_Z (GeV)	2.4947 ± 0.0026	2.4974	2.4881	± 0.0015
σ_0^{had} (nb)	41.489 ± 0.055	41.476	41.483	± 0.003
R_{had}	20.783 ± 0.029	20.753	20.725	± 0.002
R_b	0.2169 ± 0.0009	0.2156	0.2157	± 0.0002
R_c	0.1732 ± 0.0048	0.1724	0.1723	± 0.0001
$A_{\rm FB}^{\ell}$	0.0177 ± 0.0010	0.0170	0.0144	± 0.0003
$A_{\rm FB}^{b}$	0.0979 ± 0.0022	0.1056	0.0970	± 0.0010
$A_{\rm FB}^{c}$	0.0739 ± 0.0048	0.0756	0.0689	± 0.0008
A_b	0.898 ± 0.050	0.9340	0.9350	± 0.0001
A_c	0.649 ± 0.058	0.6696	0.6638	± 0.0006
ρ_ℓ	1.0039 ± 0.0013	1.0056	1.0036	± 0.0006
s_ℓ^2	0.23153 ± 0.00022	0.23114	0.23264	± 0.0002
M_W (GeV)	80.43 ± 0.08	80.417	80.219	± 0.038

electroweak corrections by 3 standard deviations. The importance of bosonic corrections is visible in the quantity s_e^2, see Figure 2. The deviation from the Standard Model prediction in the quantity R_b has been reduced to one standard deviation by now (see Figure 4). Other small deviations are observed in the asymmetries: the purely leptonic $A_{\rm FB}$ is slightly higher than the standard model predictions, and $A_{\rm FB}$ for b quarks is lower. Whereas the leptonic $A_{\rm FB}$ favors a very light Higgs boson, the b quark asymmetry needs a heavy Higgs. The measured asymmetries deviate from the best fit values by 2-3 standard deviations.

The W mass prediction in table 5 is obtained by Eq. (84) from M_Z, G_μ, α and M_H, m_t. The indirect determination of the W mass from the global fit to the LEP1/SLD data [6] (see below)

$$M_W = 80.323 \pm 0.042\,\text{GeV}\,,$$

is slightly lower, but still in agreement with the direct measurement (see table 5).

6.2. Standard model global fits

In the meantime the data have reached an accuracy such that global fits with respect to both m_t and M_H as free parameters have become available [84, 85]. The results of ref. [6] based on the most recent LEP (still preliminary) and SLD data are

$$m_t = 156^{+11}_{-9}\,\text{GeV}, \quad M_H = 39^{+63}_{-20}\,\text{GeV}\,.$$

Without the Tevatron constraint on the top mass, the favored range for m_t is a bit lower than the direct measurement. The reason for this behaviour is the strong impact on the upper limit of m_t from the quantity R_b (see Figure 4).

Together with the top mass as an additional experimental data point, the global fit to all electroweak results from LEP, SLD, M_W, νN and m_t yields the following results [6] for m_t and α_s

$$m_t = 173.3 \pm 5.4\,\text{GeV}, \quad \alpha_s = 0.120 \pm 0.003$$

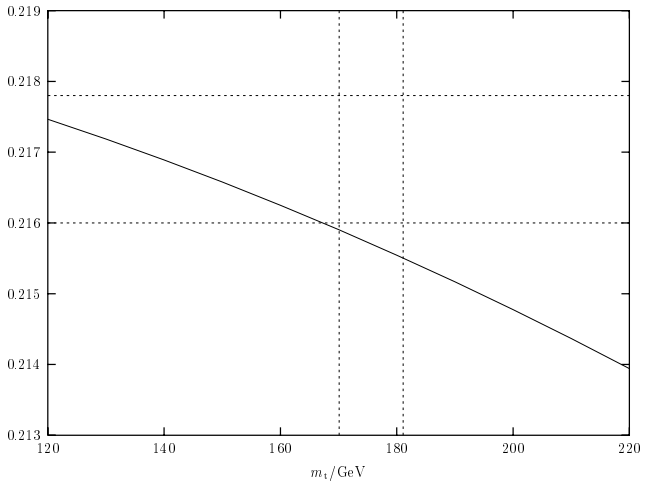

Figure 4. R_b prediction from the standard model with experimental $\pm 1\sigma$ ranges for m_t and R_b.

and for the Higgs mass:

$$M_H = 121^{+119}_{-68}\,\mathrm{GeV}\,.$$

The quality of the global fit is reflected in the χ^2/degrees of freedom = 21/15. The input from A_{LR} is decisive for a restrictive upper bound for M_H. Without A_{LR}, the 95% C.L upper bound is shifted upwards by about 260 GeV [85]. The value obtained for α_s is in very good agreement with the world average [82].

The numbers given above do not yet include the theoretical uncertainties of the standard model predictions. The LEP-EWWG [6] has performed a study of the influence of the various 'options' discussed in section 5.5 on the bounds for the Higgs mass with the result that the 95% C.L. upper bound is shifted by nearly 100 GeV to higher values, yielding

$$M_H < 430\,\mathrm{GeV}\,(95\%\ \mathrm{C.L.})\,.$$

It has to be kept in mind, however, that this error estimate is based on the uncertainties as given in table 1. Since the recent improvement in the theoretical prediction [59] is going to reduce the theoretical uncertainty one may expect also a significant smaller theoretical error on the Higgs mass bounds once the 2-loop terms $\sim G_\mu^2 m_t^2 M_Z^2$ are implemented in the codes used for the fits. At the present stage the analysis is done wwithout the new terms.

7. Conclusions

Experiments have measured the electroweak observables of the W and Z bosons and the top quark with an impressive accuracy thus providing precision tests of the electroweak theory at a level which had never been reached before. For the interpretation of the precision experiments quantum effects play a crucial role. The calculation of radiative corrections has been well established over the last years

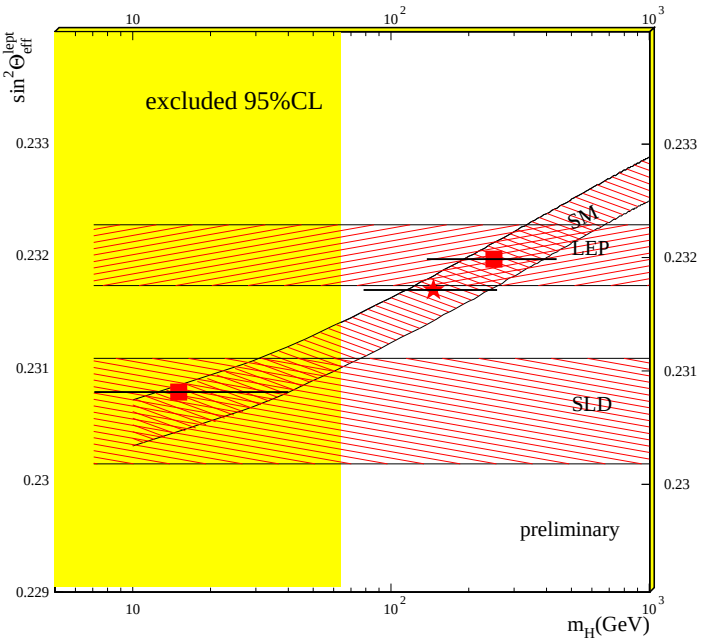

Figure 5. Dependence of the leptonic mixing angle on the Higgs mass. The theoretical predictions correspond to $m_t = 175 \pm 6$ GeV. The SLD and LEP measurements are separately shown. The star is the result of a combined fit to LEP and SLD data, the squares are for separate fits (from ref. [85])

improving and stabilizing the Standard Model predictions. LEP has provided the mass of the Z boson as the third highly accurate input parameter, besides α and G_μ, for completion of the input; each other precision observable provides a test of the electroweak theory. The theoretical predictions of the Standard Model are sensitive to the mass of the top quark and to the as yet experimentally unknown Higgs boson through the virtual presence of these particles in the loops. As a consequence, precision data can be used to pin down the allowed range of the mass parameters, yielding m_t in good agreement with the directly measured value. Although the dependence on the Higgs mass is only logarithmic, the experimental precision has reached a level where the sensitivity to M_H becomes visible, with preference for a light Higgs well below the non-perturbative regime. For the future, the reduction of the theoretical uncertainties and more precise data for M_W, m_t and $\sin^2\theta_e$ will be important entries improving the indirect Higgs search. For extracting the most precise value of M_W at LEP 2, an enormous amount of theoretical work has been provided for getting the subtleties of W pair production with the 4-fermion background under control (see [86] for a review).

Theoretical uncertainties in the Standard Model predictions have their origin essentially in the uncertainties of the hadronic vacuum polarization of the photon and from the unknown higher order contributions. In order to reach a theoretical accuracy at the level 0.1% or below, new experimental data on $\Delta\alpha$ and more complete

electroweak 2-loop calculations are required.

Quite impressive from the present point of view is the overall agreement between theory and experiment for the entire set of precision observables. The few observed deviations reduce the quality of the Standard Model fits significantly. Whether they can be understood as first signals from physics beyond the minimal model, although not very likely, is an open question at the moment.

References

[1] S.L. Glashow, *Nucl. Phys.* **B22** (1961) 579;
S. Weinberg, *Phys. Rev. Lett.* **19** (1967) 1264;
A. Salam, in: *Proceedings of the 8th Nobel Symposium*, p. 367, ed. N. Svartholm, Almqvist and Wiksell, Stockholm 1968

[2] S.L. Glashow, I. Iliopoulos, L. Maiani, *Phys. Rev.* **D2** (1970) 1285;

[3] N. Cabibbo, *Phys. Rev. Lett.* **10** (1963) 531;
M. Kobayashi, K. Maskawa, *Prog. Theor. Phys.* **49** (1973) 652

[4] H.Y. Han, Y. Nambu, *Phys. Rev.* **139** (1965) 1006;
C. Bouchiat, I. Iliopoulos, Ph. Meyer, *Phys. Lett.* **B138** (1972) 652

[5] G. 't Hooft, *Nucl. Phys.* **B33** (1971) 173; *Nucl. Phys.* **B35** (1971) 167

[6] The LEP Collaborations ALEPH, DELPHI,L3, OPAL, the LEP Electroweak Working Group and the SLD Heavy Flavor Working Group, CERN-PPE/96-183 (1996);
for the update see: J. Timmermans, talk at the *XVIII International Symposium on Lepton-Photon Interactions*, Hamburg 1997 (to appear in the proceedings)

[7] UA2 Collaboration, J. Alitti et al., *Phys. Lett.* **B276** (1992) 354;
CDF Collaboration, F. Abe et al., *Phys. Rev. Lett.* **65** (1990) 2243; *Phys. Rev.* **D43** (1991) 2070; *Phys. Rev. Lett.* **75** (1995) 11; *Phys. Rev.* **D52** (1995) 4784;
A. Gordon, talk at the XXXII Rencontre de Moriond on *Electroweak Interactions*, Les Arcs, March 1997 (to appear in the proceedings);
D0 Collaboration, S. Abachi et al., FERMILAB-PUB-96/177-E;
Y.Y. Kim, talk at the *XVIII International Symposium on Lepton-Photon Interactions*, Hamburg 1997 (to appear in the proceedings)

[8] CDF Collaboration, F. Abe et al., *Phys. Rev. Lett.* **74** (1995) 2626;
D0 Collaboration, S. Abachi et al., *Phys. Rev. Lett.* **74** (1995) 2632;
J. Lys (CDF Collaoration), in: Proceedings of the *28th International Conference on High Energy Physics*, Warsaw 1996, eds. Z. Ajduk, A.K. Wroblewski
S. Protopopescu (D0 Collaboration) in: Proceedings of the *28th International Conference on High Energy Physics*, Warsaw 1996, eds. Z. Ajduk, A.K. Wroblewski

[9] *Reports of the Working Group on Precision Calculations for the Z Resonance*, CERN 95-03 (1995), eds. D. Bardin, W. Hollik, G. Passarino

[10] Particle Data Group, R.M. Barnett et al., *Phys. Rev.* **D54** (1996) 1

[11] A. Denner, T. Sack, *Nucl. Phys.* **B347** (1990) 203

[12] C. Bollini, J. Giambiagi *Nuovo Cim.* **12B** (1972) 20;
J. Ashmore, *Nuovo Cim. Lett.* **4** (1972) 289;
G. 't Hooft, M. Veltman, *Nucl. Phys.* **B44** (1972) 189

[13] G. Passarino, in: *Proceeedings of the LP-HEP 91 Conference*, Geneva 1991, eds. S. Hegarty, K. Potter, E. Quercigh, World Scientific, Singapore 1992

[14] G. Passarino, *Phys. Lett.* **B231** (1989) 458; *Phys. Lett.* **B247** (1990) 587; *Nucl. Phys.* **B361** (1991) 351

[15] G. 't Hooft, *Nucl. Phys.* **B61** (1973) 455; *Nucl. Phys.* **B62** (1973) 444

[16] D.A. Ross, J.C. Taylor, *Nucl. Phys.* **B51** (1973) 25

[17] G. Passarino, M. Veltman, *Nucl. Phys.* **B160** (1979) 151

[18] M. Consoli, *Nucl. Phys.* **B160** (1979) 208

[19] A. Sirlin, *Phys. Rev.* **D22** (1980) 971;
W. J. Marciano, A. Sirlin, *Phys. Rev.* **D22** (1980) 2695;
A. Sirlin, W. J. Marciano, *Nucl. Phys.* **B189** (1981) 442

[20] D.Yu. Bardin, P.Ch. Christova, O.M. Fedorenko, *Nucl. Phys.* **B175** (1980) 435; *Nucl. Phys.* **B197** (1982) 1;
D.Yu. Bardin, M.S. Bilenky, G.V. Mithselmakher, T. Riemann, M. Sachwitz, *Z. Phys.* **C44** (1989) 493

[21] J. Fleischer, F. Jegerlehner, *Phys. Rev.* **D23** (1981) 2001
[22] K.I. Aoki, Z. Hioki, R. Kawabe, M. Konuma, T. Muta, *Suppl. Prog. Theor. Phys.* **73** (1982) 1; Z. Hioki, *Phys. Rev. Lett.* **65** (1990) 683, E:1692; *Z. Phys.* **C49** (1991) 287
[23] M. Consoli, S. LoPresti, L. Maiani, *Nucl. Phys.* **B223** (1983) 474
[24] D.Yu. Bardin, M.S. Bilenky, G.V. Mithselmakher, T. Riemann, M. Sachwitz, *Z. Phys.* **C44** (1989) 493
[25] M. Böhm, W. Hollik, H. Spiesberger, *Fortschr. Phys.* **34** (1986) 687
[26] W. Hollik, *Fortschr. Phys.* **38** (1990) 165
[27] M. Consoli, W. Hollik, F. Jegerlehner, in: *Z Physics at LEP 1*, eds. G. Altarelli, R. Kleiss and C. Verzegnassi, CERN 89-08 (1989)
[28] G. Passarino, R. Pittau, *Phys. Lett.* **B228** (1989) 89; V.A. Novikov, L.B. Okun, M.I. Vysotsky, CERN-TH.6538/92 (1992)
[29] M. Veltman, *Phys. Lett.* **B91** (1980) 95; M. Green, M. Veltman, *Nucl. Phys.* **B169** (1980) 137, E: *Nucl. Phys.* **B175** (1980) 547; F. Antonelli, M. Consoli, G. Corbo, *Phys. Lett.* **B91** (1980) 90; F. Antonelli, M. Consoli, G. Corbo, O. Pellegrino, *Nucl. Phys.* **B183** (1981) 195
[30] G. Passarino, M. Veltman, *Phys. Lett.* **B237** (1990) 537
[31] W.J. Marciano, A. Sirlin, *Phys. Rev. Lett.* **46** (1981) 163; A. Sirlin, *Phys. Lett.* **B232** (1989) 123
[32] G. Degrassi, S. Fanchiotti, A. Sirlin, *Nucl. Phys.* **B351** (1991) 49
[33] G. Degrassi, A. Sirlin, *Nucl. Phys.* **B352** (1991) 342
[34] D.C. Kennedy, B.W. Lynn, *Nucl. Phys.* **B322** (1989) 1
[35] M. Kuroda, G. Moultaka, D. Schildknecht, *Nucl. Phys.* **B350** (1991) 25
[36] L.D. Faddeev, V.N. Popov, *Phys. Lett.* **B25** (1967) 29
[37] S. Willenbrock, G. Valencia, *Phys. Lett.* **B259** (1991) 373; R. Stuart, *Phys. Lett.* **B262** (1991) 113; A. Sirlin, *Phys. Rev. Lett.* **67** (1991) 2127
[38] J.C. Ward, *Phys. Rev.* **78** (1950) 1824
[39] D. Ross, M. Veltman, *Nucl. Phys.* **B95** (1975) 135; M. Veltman, *Nucl. Phys.* **B123** (1977) 89;
[40] M.S. Chanowitz, M.A. Furman, I. Hinchliffe, *Phys. Lett.* **B78** (1978) 285
[41] M. Veltman, *Acta Phys. Polon.* **B8** (1977) 475.
[42] R.E Behrends, R.J. Finkelstein, A. Sirlin, *Phys. Rev.* **101** (1956) 866; T. Kinoshita, A. Sirlin, *Phys. Rev.* **113** (1959) 1652
[43] S. Eidelman, F. Jegerlehner, *Z. Phys.* **C67** (1995) 585
[44] H. Burkhardt, B. Pietrzyk, *Phys. Lett.* **B356** (1995) 398
[45] F. Jegerlehner, *Progress in Particle and Nuclear Physics* **27** (1991) 1, updated from: H. Burkhardt, F. Jegerlehner, G. Penso, C. Verzegnassi, *Z. Phys.* **C43** (1989) 497;
[46] M.L. Swartz, *Phys. Rev.* **D53** (1996) 5268
[47] A.D. Martin, D. Zeppenfeld, *Phys. Lett.* **B345** (1995) 558
[48] R. Alemany, M. Davier, A. Höcker, hep-ph/9703220
[49] W.J. Marciano, *Phys. Rev.* **D20** (1979) 274
[50] M. Consoli, W. Hollik, F. Jegerlehner, *Phys. Lett.* **B227** (1989) 167.
[51] J.J. van der Bij, F. Hoogeveen, *Nucl. Phys.* **B283** (1987) 477
[52] R. Barbieri, M. Beccaria, P. Ciafaloni, G. Curci, A. Vicere, *Phys. Lett.* **B288** (1992) 95; *Nucl. Phys.* **B409** (1993) 105; J. Fleischer, F. Jegerlehner, O.V. Tarasov, *Phys. Lett.* **B319** (1993) 249
[53] A. Djouadi, *Nuovo Cim.* **100A** (1988) 357; D. Yu. Bardin, A.V. Chizhov, Dubna preprint E2-89-525 (1989); B.A. Kniehl, *Nucl. Phys.* **B347** (1990) 86; F. Halzen, B.A. Kniehl, *Nucl. Phys.* **B353** (1991) 567; A. Djouadi, P. Gambino, *Phys. Rev.* **D49** (1994) 3499
[54] A. Djouadi, C. Verzegnassi, *Phys. Lett.* **B195** (1987) 265
[55] L. Avdeev, J. Fleischer, S. M. Mikhailov, O. Tarasov, *Phys. Lett.* **B336** (1994) 560; E: *Phys. Lett.* **B349** (1995) 597; K.G. Chetyrkin, J.H. Kühn, M. Steinhauser, *Phys. Lett.* **B351** (1995) 331
[56] B.A. Kniehl, J.H. Kühn, R.G. Stuart, *Phys. Lett.* **B214** (1988) 621; B.A. Kniehl, A. Sirlin, *Nucl. Phys.* **B371** (1992) 141; *Phys. Rev.* **D47** (1993) 883; S. Fanchiotti, B.A. Kniehl, A. Sirlin, *Phys. Rev.* **D48** (1993) 307
[57] K.G. Chetyrkin, J.H. Kühn, M. Steinhauser, *Phys. Rev. Lett.* **75** (1995) 3394
[58] A. Sirlin, *Phys. Rev.* **D29** (1984) 89

[59] G. Degrassi, P. Gambino, A. Vicini, *Phys. Lett.* **B383** (1996) 219;
G. Degrassi, P. Gambino, A. Sirlin, *Phys. Lett.* **B394** (1997) 188
[60] S. Bauberger, G. Weiglein, *Nucl. Instrum. Meth.* **A389** (1997) 318; ——hep-ph/9707510
[61] G.L. Fogli and D. Haidt, *Z. Phys.* **C40** (1988) 379;
CDHS Collaboration, H. Abramowicz et al., *Phys. Rev. Lett.* **B57** (1986) 298; A. Blondel et al, *Z. Phys.* **C45** (1990) 361;
CHARM Collaboration, J.V. Allaby et al., *Phys. Lett.* **B177** (1987) 446;
Z. Phys. **C36** (1987) 611;
CHARM-II Collaboration, D. Geiregat et al., *Phys. Lett.* **B247** (1990) 131;
Phys. Lett. **B259** (1991) 499;
CCFR Collaboration, C.G. Arroyo et al., *Phys. Rev. Lett.* **72** (1994) 3452;
K. McFarlane (CCFR Collaboration), in: Proceedings of the *28th International Conference on High Energy Physics*, Warsaw 1996, eds. Z. Ajduk, A.K. Wroblewski
[62] C.H. Llewellyn Smith, *Nucl. Phys.* **B228** (1983) 205
[63] A.A. Akhundov, D. Bardin, T. Riemann, *Nucl. Phys.* **B276** (1986) 1;
W. Beenakker, W. Hollik, *Z. Phys.* **C40** (1988) 141;
J. Bernabeu, A. Pich, A. Santamaria, *Phys. Lett.* **B200** (1988) 569; *Nucl. Phys.* **B363** (1991) 326
[64] A. Denner, W. Hollik, B. Lampe, *Z. Phys.* **C60** (1993) 93
[65] J. Fleischer, O.V. Tarasov, F. Jegerlehner, P. Rączka, *Phys. Lett.* **B293** (1992) 437;
G. Buchalla, A.J. Buras, *Nucl. Phys.* **B398** (1993) 285;
G. Degrassi, *Nucl. Phys.* **B407** (1993) 271;
K.G. Chetyrkin, A. Kwiatkowski, M. Steinhauser, *Mod. Phys. Lett.* **A8** (1993) 2785
[66] A. Kwiatkowski, M. Steinhauser, *Phys. Lett.* **B344** (1995) 359;
S. Peris, A. Santamaria, *Nucl. Phys.* **B445** (1995) 252
[67] F.A. Berends et al., in: *Z Physics at LEP 1*, CERN 89-08 (1989), eds. G. Altarelli, R. Kleiss, C. Verzegnassi, Vol. I, p. 89;
W. Beenakker, F.A. Berends, S.C. van der Marck, *Z. Phys.* **C46** (1990) 687
[68] A. Borelli, M. Consoli, L. Maiani, R. Sisto, *Nucl. Phys.* **B333** (1990) 357
[69] G. Burgers, F.A. Berends, W. Hollik, W.L. van Neerven, *Phys. Lett.* **B203** (1988) 177
[70] D. Yu. Bardin, A. Leike, T. Riemann, M. Sachwitz, *Phys. Lett.* **B206** (1988) 539
[71] G. Burgers, F.A. Berends, W.L.van Neerven, *Nucl. Phys.* **B297** (1988) 429; E: *Nucl. Phys.* **B304** (1988) 921;
W. Beenakker, F.A. Berends, S.C. van der Marck, *Z. Phys.* **C46** (1990) 687
[72] K.G. Chetyrkin, A.L. Kataev, F.V. Tkachov, *Phys. Lett.* **B85** (1979) 277;
M. Dine, J. Sapirstein, *Phys. Rev. Lett.* **43** (1979) 668;
W. Celmaster, R. Gonsalves, *Phys. Rev. Lett.* **44** (1980) 560;
S.G. Gorishny, A.L. Kataev, S.A. Larin, *Phys. Lett.* **B259** (1991) 144;
L.R. Surguladze, M.A. Samuel, *Phys. Rev. Lett.* **66** (1991) 560;
A. Kataev, *Phys. Lett.* **B287** (1992 209
[73] A. Czarnecki, J.H. Kühn, *Phys. Rev. Lett.* **77** (1996) 3955
[74] For a review see: K.G. Chetyrkin, J.H. Kühn, A. Kwiatkowski, in [82], p. 175; *Phys. Rep.* **277** (1996) 189
[75] J.H. Kühn, B.A. Kniehl, *Phys. Lett.* **B224** (1990) 229;
Nucl. Phys. **B329** (1990) 547
[76] A. Hoang, J.H. Kühn, T. Teubner, *Nucl. Phys.* **B455** (1995) 3; **B452** (1995) 173
[77] M. Böhm, W. Hollik *Nucl. Phys.* **B204** (1982) 45; *Z. Phys.* **C 23** (1984) 31
[78] S. Jadach, J.H. Kühn, R.G. Stuart, Z. Wąs, *Z. Phys.* **C38** (1988) 609;
J.H. Kühn, R.G. Stuart, *Phys. Lett.* **B200** (1988) 360
[79] M. Böhm, W. Hollik et al., in: *Z Physics at LEP 1*, CERN 89-08 (1989), eds. G. Altarelli, R. Kleiss, C. Verzegnassi, Vol. I, p. 203;
J.H. Kühn, P.Zerwas et al., in: *Z Physics at LEP 1*, CERN 89-08 (1989), eds. G. Altarelli, R. Kleiss, C. Verzegnassi, Vol. I, p. 267
[80] B.A. Kniehl, in [82], p. 299
[81] D. Bardin et al., in [82], p. 7
[82] M. Schmelling, in: Proceedings of the *28th International Conference on High Energy Physics*, Warsaw 1996, eds. Z. Ajduk, A.K. Wroblewski
[83] SLD Collaboration, P. Rowson, talk at the XXXII Rencontre de Moriond on *Electroweak Interactions*, Les Arcs, March 1997 (to appear in the Proceedings)
[84] K. Hagiwara, D. Haidt, S. Matsumoto, KEK-TH-512, DESY 96-192, hep-ph/9706331;
J. Ellis, G.L. Fogli, E. Lisi, *Phys. Lett.* **B389** (1996) 321; *Z. Phys.* **C69** (1996) 627;

G. Passarino, *Acta Phys. Polon.* **B28** (1997) 635;
S. Dittmaier, D. Schildknecht, *Phys. Lett.* **B391** (1997) 420;
S. Dittmaier, D. Schildknecht, G. Weiglein, *Phys. Lett.* **B386** (1996) 247;
P. Chankowski, S. Pokorski, *Acta Phys. Polon.* **27** (1996) 1719
[85] W. de Boer, A. Dabelstein, W. Hollik, W. Mösle, U. Schwickerath, hep-ph/9609209 (to appear in Z. Phys. C)
[86] Physics at LEP 2, CERN 96-01 (1996), eds. D. Altarelli, T. Sjostrand, F. Zwirner